iScience

CellPress
OPEN ACCESS

Review

Magnetically active lithium-ion batteries towards battery performance improvement

Carlos M. Costa,[1,2,*] Karla J. Merazzo,[3] Renato Gonçalves,[4] Charles Amos,[5] and Senentxu Lanceros-Méndez[3,6,*]

SUMMARY

Lithium-ion batteries (LIBs) are currently the fastest growing segment of the global battery market, and the preferred electrochemical energy storage system for portable applications. Magnetism is one of the forces that can be applied improve performance, since the application of magnetic fields influences electrochemical reactions through variation of electrolyte properties, mass transportation, electrode kinetics, and deposits morphology. This review provides a description of the magnetic forces present in electrochemical reactions and focuses on how those forces may be taken advantage of to influence the LIBs components (electrolyte, electrodes, and active materials), improving battery performance. The different ways that magnetic forces can interact with LIBs components are discussed, as well as their influence on the electrochemical behavior. The suitable control of these forces and interactions can lead to higher performance LIBs structures and to the development of innovative concepts.

INTRODUCTION

Energy and environment will continue to be the top priorities of global society in the years to come. Radical changes in the world's energy mix are required to move toward a more sustainable, environmentally friendly future, while maintaining critical, energy-intensive industries. One energy source that needs to be reduced is petroleum. Fossil fuel usage should be strongly curbed to properly address climate change (Nejat et al., 2015). As a substitute energy storage technology, lithium-ion batteries (LIBs) can play a crucial role in displacing fossil fuels without emitting greenhouse gases, as they efficiently store energy for long periods of time in applications ranging from portable electronic devices to electric vehicles (Nitta et al., 2015). Despite the success of LIBs, further advancements in the properties and performance of their components (electrodes, separator, electrolyte) are needed (Scrosati et al., 2011).

Battery electrodes can be separated into anodes (negative electrodes) and cathodes (positive electrodes). The lowest capacity electrode (typically the cathode) determines the overall capacity of a battery. Different types/structures are applied for the separator component, which mainly serves to physically separate the electrodes to prevent shorting while providing porosity for lithium ion transport during charge and discharge (Costa et al., 2013, 2019). The most widely used materials for anodes are carbon-based, whereas the most widely used materials for the cathode are transition metal-based intercalation materials (layered oxides, spinel oxides, and olivine phosphates) (Hayner et al., 2012). Transition metals, typically Mn, Fe, Co, and/or Ni, allow for the cathodes to be particularly designed to make use of their magnetic properties (Chernova et al., 2011).

There are several examples of batteries that use the benefits of magnetic fields (MFs) and studies of the physical phenomena that occur because of magnetic interactions. A patent was granted in 1987 for the concept of magnetic batteries, which included a helical spring threaded onto a magnetic core and hence electricity was extracted therefrom (Ridley and Spector, 1987). In another work, an approximately 100% in the electrochemical mass transport was demonstrated when MFs of about 1 T were applied to aqueous electrolytes (Hinds et al., 2001a). The effect of an applied MF on the function of an electrochemical cell has been also studied (Aogaki et al., 1994; Nyman, 2011) to address the main physical phenomena that can influence battery performance. One of the most relevant effects that occurs when MFs are applied to an electrochemical cell is the magnetohydrodynamic (MHD) effect (O'Brien, 2019), which describes the motion of a conductive fluid flowing in the presence of an externally applied MF. The main concept is

[1]Centre of Physics, University of Minho, 4710-057 Braga, Portugal

[2]Institute of Science and Innovation for Bio-Sustainability (IB-S), University of Minho, 4710-053 Braga, Portugal

[3]BCMaterials, Basque Center for Materials, Applications and Nanostructures, UPV/EHU Science Park, 48940 Leioa, Spain

[4]Centre of Chemistry, University of Minho, 4710-057 Braga, Portugal

[5]INL- International Iberian Nanotechnology Laboratory, 4715-330 Braga, Portugal

[6]IKERBASQUE, Basque Foundation for Science, 48009 Bilbao, Spain

*Correspondence: cmscosta@fisica.uminho.pt (C.M.C.), senentxu.lanceros@bcmaterials.net (S.L.-M.)

https://doi.org/10.1016/j.isci.2021.102691

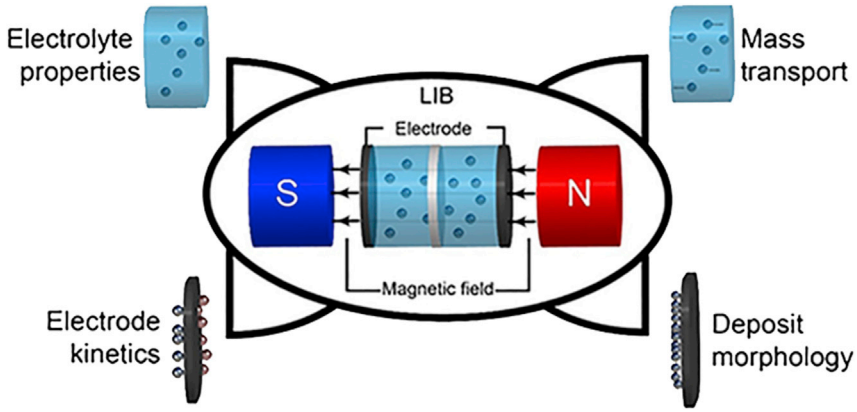

Figure 1. Schema of the possible effects of an applied magnetic field on electrochemical reactions, particularly for a battery.

that MFs induce current variations in a flowing, conductive fluid, which polarizes the fluid and correspondingly changes the MF. Another phenomenon that may occur is magnetoelectrolysis (Aogaki et al., 1994), which is the decomposition of one or several chemical species by electric current influenced by an applied MF. The main advantage of carrying out electrolysis within a MF is the achievement of substantial mass transport rates. This effect is particularly important in the electrodeposition of metals. With proper electric/MF arrangements, the quality of the deposit can be maintained even with large current densities.

A MF influences electrochemical reactions in different ways, generalized below into various categories (Figure 1) (Aogaki et al., 1994):

- Modified electrolyte properties: Hall Effect and electrical conductivity variations under applied MFs.
- Modified mass transport: superposition of the MF may be primarily attributed to an interaction of MHD phenomena and the convective diffusion layer near the electrodes.
- Electrode kinetics (or electrochemical kinetics) variations under MF.
- Deposit morphology: variations on deposit quality in magnetoelectrolysis (Fahidy, 1983).

Without an applied field, the dominant driving forces in the electrolyte component are electromigration, diffusion, and convection, both natural and forced (for the case of a rotating disk electrode). With an applied MF, there are five additional forces, which can lead to the MF effects that are observed: field gradient, paramagnetic gradient, electrokinetic, Lorentz, and magnetic damping in the electrical conductivity (Grant et al., 1999; Hinds et al., 2001a). All five forces are body forces with units N/m^3, and in electrolyte-induced variations, both magnitude and direction are relevant.

By tailoring the experimental conditions in aqueous electrodes, magnetic body forces such as Lorentz (F_L), electrokinetic (F_E), and MF gradient (F_B), might present equivalent magnitude. When a uniform MF is applied, the F_B force is nonexistent, however F_L and F_E induce convection. The paramagnetic gradient force (F_P) is a sizable magnetic force when compared with other magnetic forces that could be present and, due to the cation concentration gradient, is responsible for field effects in paramagnetic solutions. However, this force does not substantially influence mass transport, its effect on battery performance being negligible when compared to the forces that drive diffusion (F_D). A similar situation occurs with the magnetic damping force (F_M), the effect of which is negligible since the transverse flow is opposed by a force (Hinds et al., 2001a).

All those effects induce complex effects in the LIB response; therefore, this review focuses on clarifying how each effect, depending on MF and magnetic properties, influences the operation of an LIB to take advantage of the MF induced effects to improve battery performance. It is to notice that related effects can be applied to other energy storage systems with MF sensitive materials and/or processes.

Magnetic forces present in the components of a battery

The paramagnetic gradient force (F_P) and the field gradient force (F_B) are the principal driving forces created by a magnetic energy gradient, depending on the magnetic properties of the electrolyte.

- F_P: The paramagnetic gradient force arises from differences in the paramagnetic susceptibility within the diffusion layer caused by the cation concentration gradient. The magnitude of this force may be much less than the driving force for diffusion.
- F_B: Field gradient force is more significant when compared to the paramagnetic gradient force. It is a result of a non-uniform MF in solution, which can arise near the surface of a rough ferromagnetic electrode, for example.

The electrolyte energy influenced by a MF is expressed as:

$$E_{mag} = -\left(\frac{1}{2}\right) MB \left[J/m^3\right] \quad \text{(Equation 1)}$$

where $M = X_m cB$ - represents the magnetization (A/m) induced by the MF B (T). X_m and c represent the molar susceptibility and concentration, respectively. According to that, it is obtained:

$$E_{mag} = -\left(\frac{1}{2\mu_0}\right) \frac{X_m cB^2}{\mu_0} \quad \text{(Equation 2)}$$

$$\overrightarrow{F}_{mag} = -\overrightarrow{\nabla} E_{mag} \quad \text{(Equation 3)}$$

$$\overrightarrow{F}_{mag} = \frac{X_m B^2 \overrightarrow{\nabla} c}{2\mu_0} + \frac{X_m cB \overrightarrow{\nabla} B}{\mu_0} = \overrightarrow{F}_P + \overrightarrow{F}_B \quad \text{(Equation 4)}$$

where $\overrightarrow{F}_P = \frac{X_m B^2 \overrightarrow{\nabla} c}{2\mu_0}$, represent the paramagnetic gradient force and $\overrightarrow{F}_B = \frac{X_m cB \overrightarrow{\nabla} B}{\mu_0}$ the field gradient force.

F_P is responsible for the MF effects in paramagnetic solutions (O'Brien and Santhanam, 1997), and its effect becomes more pronounced in the diffusion layer at the electrode/electrolyte interphase. As mentioned previously, it arises from the gradient in magnetic susceptibility caused by the concentration gradient of paramagnetic ions near the electrode's surface (Hinds et al., 2001a). The thermodynamic driving force for diffusion is approximately 10^{-6} times higher than the F_P at room temperature, therefore, it is expected that this force has a negligible effect on mass transport (Hinds et al., 2001a).

The field gradient force (F_B) may become substantial in non-uniform MFs, at the macroscale or microscale of the whole cell or at the surface of ferromagnetic electrodes, respectively. At typical experimental conditions, the field gradient force is of the order of $10\ N \cdot m^{-3}$ (~1% of the Lorentz force). F_B can become dominant when a field gradient is applied intentionally ($\nabla B \gg 1$ T/m) (Leventis and Gao, 2002). Mohanta et al. (Mohanta and Fahidy, 1978) reported that a convective-diffusion layer at the electrodes is predominant in non-uniform fields under MFs.

Two other forces related to the interaction of the MF and the electric current due to the flux of ions:

3. Lorentz force (F_L) occurs when the MF (B) and current density (j) are nonparallel, the effect of which is an induced flow in the electrolyte when it is perpendicular to the current direction. It significantly affects the diffusion limited current during an electrode process (Figure 2).

The Lorentz force (Equation 5) is expressed as

$$F_L = \overrightarrow{j} \times \overrightarrow{B} = q\left(E + v_d \times B\right) \quad \text{(Equation 5)}$$

where E is the electric field, velocity (v_d) of charge (q) across lines of magnetic flux (B).

4. The electrokinetic force (S_E), Equation 6, is defined as the force acting on charges in the diffuse double layer under the effect of a dynamic electric field, $\overrightarrow{E}_{\|}$, parallel to the electrode's surface.

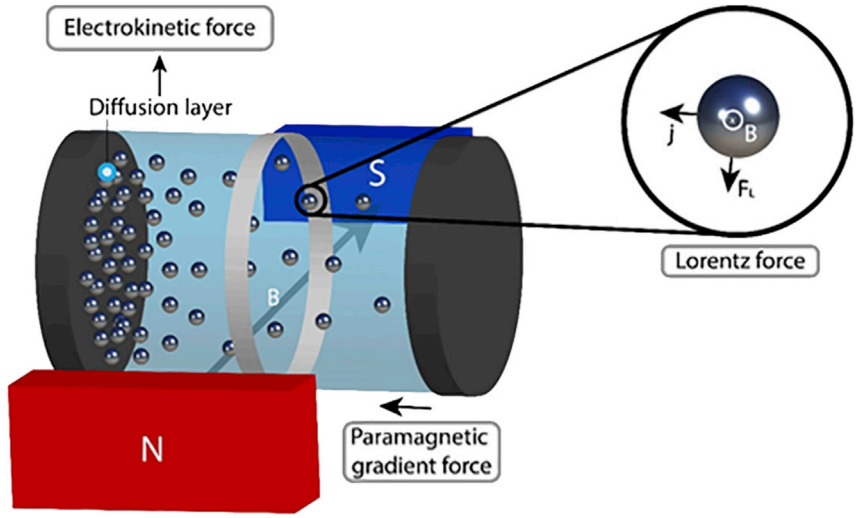

Figure 2. Magnetic-related forces on charges moving through a magnetic field.

$$\vec{S}_E = \sigma_d \vec{E}_{\parallel} \quad \text{(Equation 6)}$$

where σ_d (C/m^2) represents the charge density of the diffuse double layer and $\vec{E}_{\parallel}$, is an effective electric field representing the interaction of charges moving across the double layer under the influence of a MF applied parallel to the electrode surface.

Such an applied MF may be created through the direct application of a MF to the electrode surface or by means of a tangential electric field close to the electrode surface (Olivier et al., 2000), using a sweeping potential working electrode for example. In the charge density, σ_d, within the diffuse double layer, the electrokinetic stress, S_E, stimulates a tangential flow, which is driven to the bulk solution by viscous forces. The electrokinetic stress can be compared with other body forces by dividing with a characteristic length, χ, that scales with the dimensions of the hydrodynamic boundary layer, δ_0, and dividing per unit area, in this case a few nanometers considering the scale of the action of the electrode surface. Taking $\chi \approx 1$ nm and scaling by a factor χ/δ_0 yields $F_E \approx 10^3$ N/m^3, an equivalent order of magnitude to that of the Lorentz force. The origin of these forces is equivalent; the main difference being the length scale on which they work. Does the microscopic flow drive the macroscopic flow or vice versa? Considering that these forces are equivalent in magnitude, it is probable that both forces show approximately a similar role in the interaction between the flows at the micro- and macroscopic levels. These forces must be factored into the quantitative analysis related to the increase in mass transport induced by the field.

5. Longitudinal flow of charges in the direction of the MF (*B*) is unobstructed, but transversal flow with velocity *v* is damped because of an opposing force (Equation 7).

$$\vec{F}_M = \sigma \vec{v} \times \vec{B} \times \vec{B} \quad \text{(Equation 7)}$$

where $\vec{v} \times \vec{B}$ is the non-electrostatic field resulting from the applied MF (Hinds et al., 2001a).

The magnetic damping force is significant in conducting melts such as those used in semiconductor and metal processing, but as mentioned before in low-conductivity, aqueous solutions, this force is negligible.

Within LIBs, the application of an external MF affects the solid electrolyte interphase (SEI) layer, the porous electrodes, and electrolyte decomposition reactions by varying the current density (J) (Singh et al., 2018).

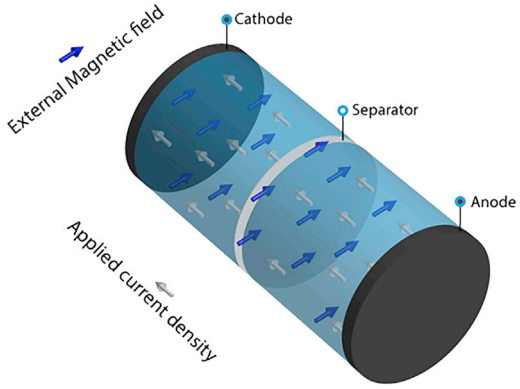

Figure 3. 3-D model geometry of a Li-ion battery under an applied magnetic field showing also the electrode current density directions (Singh et al., 2018).

COUPLING OF MFS AND LITHIUM-ION BATTERY – HALL EFFECT

The Hall Effect is the resulting transversal voltage difference in an electrical conductor in which the applied MF is perpendicular to the current (Figure 3).

The equations that explain the coupling of an external MF and the behavior of the current density are (Singh et al., 2018):

$$\text{Ampere's-Maxwell law: } \nabla \times H = J \qquad \text{(Equation 8)}$$

$$\text{Ampere's-Maxwell law: } E = \sigma^{-1} (\nabla \times H) \qquad \text{(Equation 9)}$$

$$\text{Faraday's law: } \nabla \times E = -\frac{\partial B}{\partial t} \qquad \text{(Equation 10)}$$

$$\text{Lorentz force: } F_L = q (E + v_d \times B) \qquad \text{(Equation 11)}$$

Where σ is electrical conductivity, B is magnetic flux density, H is MF, J is current density, E is electric field and movement (v_d) of charge (q)

The bidirectional coupling between an externally applied MF and the LIB leads to variations in the performance of the LIB and concurrently, the MF is affected by the condition of the LIB. In this case, the following behavior of battery components can be expected under the influence of a MF:

- Lithium-ion concentration variation, at the anode, verified during the charge/discharge processes, that influences the present external MF, due to the lithium-ions paramagnetic properties (Singh et al., 2018).
- SEI layer formation/growth due to parasitic lithium/solvent reduction growth during aging.
- Cathode active material valence change (ex. lithium metal oxide - $LiMO_2$ is converted to metal oxide - MO_2), during LIB operation, which influences the value of external MF, since the change of oxidation state of the transition metal affects its magnetic properties (Yang et al., 2002).

In the absence of a MF, Ohm's law gives current density according to the equation J = σE. In the presence of an externally applied MF, the equation for current density is modified to include the Hall Effect (Chien, 2013). The expression for current density (J) considering the Hall Effect for electrodes and the electrolyte is:

$$J = \sigma \cdot E + \frac{\sigma^2}{C_1 \cdot F} (B \times E) \qquad \text{(Equation 12)}$$

The effect of the operation of an LIB on the MF is considered in terms of a Lorentz force, which causes a change in the electric field thereby affecting the external MF (Hinds et al., 2001a). The drift velocity of the charge carriers is given as input for the Lorentz force (Miura et al., 2017):

$$v_d = \frac{\sigma \cdot \nabla \varnothing}{F \cdot C_1} \quad \text{(Equation 13)}$$

Magnetic properties of active materials

Electron spin probe magnetometry, electron paramagnetic resonance (EPR), and techniques such as nuclear magnetic resonance (NMR) and real-time X-ray absorption spectroscopy are some of the techniques that have been used to better understand ion intercalation and conversion in batteries. With the use of these techniques during battery operation, it is possible to obtain essential information such as structure, dendrite growth, magnetic interactions of redox species, failure mechanisms, electron spins and defects (Nguyen and Clément, 2020; Pecher et al., 2017). Once a material's magnetic and electronic properties are correlated, a better and more detailed comprehension of the energy storage mechanisms of that material will follow. Magnetometry and EPR allow us to determine the growth of ferromagnetic particles and also verify if a conductive network is created on them, a necessary property to ensure reversibility in electron transfer process during battery operation (Nguyen and Clément, 2020).

Magnetic particles and corresponding composites, including α-Fe_2O_3 (Wu et al., 2006), Fe_3O_4 nanoparticles (Wei et al., 2017b), Co_3O_4 nanoparticle (Rahman et al., 2009), $MnFe_2O_4$ particles (Lin et al., 2013), Fe_3O_4/reduced graphene oxide (RGO) (Wang et al., 2016), W-doped Fe_3O_4 (Guo et al., 2013), $FeSn_2$ nanocrystals (Nwokeke et al., 2011), $Fe_{2\text{-}y}PO_4(OH)$ (Song et al., 2005), $Fe_{2-x}Mn_xO_3$ composite oxides (Guo et al., 2020), $MnSn_2$ material (Philippe et al., 2014), magnetic biochar (Salimi et al., 2019), magnetic tubular carbon nanofibers based on $FeCl_3$ (Huyan et al., 2019), $MnCo_2O_4$ (Duan et al., 2013), and FeSi4P4 material (Coquil et al., 2017), have been used for anodes in LIBs where their magnetic properties are essential for applications.

Graphite is widely used as active material for anodes. The magnetic susceptibility of Li-intercalated graphite compounds, C_6Li_x, was evaluated with the objective to elucidate their magnetism as a function of x (where x = 0.14, 0.25, 0.29, 0.34, 0.50, 0.61, and 1). The sample where x = 0 (pure graphite) showed a large diamagnetic response with magnetic susceptibility values at 5 K and 300 K being -127×10^{-6} emu·mol^{-1} and -67 $\times 10^{-6}$ emu·mol^{-1}, respectively. The transition from diamagnetic to paramagnetic behavior took place gradually at around $x \geq 0.34$, which contradicts the expected x dependence of the orbital magnetic susceptibility based on the tight binding model (Mukai and Inoue, 2017).

The active materials in cathodes include elements such as Fe, Ni, Co, or Mn. These materials are characterized by different magnetic properties, and their magnetic characterization is fundamental to evaluate their quality. Also, this evaluation is important to find out how magnetic material properties affect battery performance through the determination of temperature and stress dependence, ferromagnetic impurities and defects, all of which will influence their magnetic properties (e.g., magnetic susceptibility) (Huang et al., 2017; Julien et al., 2007; Zhang et al., 2011; Zheng-Fei Guo and Xue-Jin, 2016).

In $LiCoO_2$, magnetic susceptibility measurements revealed a thermally induced magnetic spin state transition from low spin to intermediate spin at ~800 K in bulk $LiCoO_2$ (Oz et al., 2017). In addition, for this active material, the temperature dependence of the magnetic susceptibility shows Pauli paramagnetic behavior, which supports the idea outlined previously that Co^{3+} ions are in a low-spin state with S = 0 (Mukai et al., 2014). In addition, weak transverse-field muon-spin rotation and relaxation (μ^+SR) spectroscopy measurements have shown that localized moments appear in $LiCoO_2$ below 60 K, while both $Li_{0.04}CoO_2$ and $Li_{0.53}CoO_2$ are paramagnetic at temperatures down to 10 K (Mukai et al., 2007).

The magnetic properties of $LiMO_2$ (where M = Ni, Co, and Mn or a mixture such as M = $Ni_{1/3}Mn_{1/3}Co_{1/3}$) were evaluated, the band gap being established by charge-transfer and the main contributions from magnetic polarons being the production of spin electron -hole pairs (Eom et al., 2017).

The magnetic characteristics of $Li_xMn_2O_4$ in the range $0.07 \leq x \leq 1$ show that the effective magnetic moment (μ_{eff}) of Mn ions decreases monotonically with decreasing x; antiferromagnetic interaction dominates in the whole of the range of x (Mukai et al., 2011). The magnetic properties of $LiNi_{1-x}Co_xO_2$ samples (x = 0, 0.05, 0.1 and 0.25) are characterized by a temperature dependence of χ^{-1} (MF H = 10 kOe), which is compatible with Curie–Weiss paramagnetic behavior to temperatures down to ~100 K. At low temperatures, all of the samples entered a spin-glass-like phase below the spin freezing temperature (T_f) (Mukai et al., 2010).

It was observed that $Li_xNi_{1/3}Mn_{1/3}Co_{1/3}O_2$ enters into a spin-glass-like magnetic state below approximately T = 12 K at lithium contents x = 1 and x = 0.3; above T_{diff} = 125 K, the lithium ions begin diffusing as indicated by an exponential increase in the hopping rate (Månsson et al., 2014).

For $LiMn_{1-x}Fe_xPO_4$ with $0 \leqslant x \leqslant 1$, antiferromagnetic interactions between the 3d-transition metal moments are observed at low temperatures (Neef et al., 2017).

In the evaluation of the magnetic properties of Li_x(Co-Ni-Mn)O_2, it was observed that magnetic moments, localized at the transition metals, appear with decreasing Li^+ content. The largest magnetic moment was calculated for Mn atoms (~ 1.5 μB), while smaller magnetic moments (~ 0.2μB) were found for Co atoms (Rybski et al., 2018). Also, for this active material, it was observed that long-range magnetic order is unobtainable, even at temperatures as low as 3 K (Xiao et al., 2018). Co substitution facilitates the ordering of Li and Ni by reducing both intra-plane magnetic frustration and inter-plane super-exchange (SE) interaction. Mn works counter to this by exacerbating magnetic frustration and strengthening SE, thereby aggravating Li/Ni mixing (Wang et al., 2019a).

A study of the magnetic properties of $Li_{1+z}(Ni_{0.45}Mn_{0.45}Co_{0.1})_{1-z}O_2$ showed that interlayer clusters nucleated at interfacial Ni^{2+} ions. It was also observed that particle size increases with increasing Ni and Li disorder and that the size of the intralayer clusters increases with larger particle size and smaller amounts of non-magnetic ions in the transition metal layers (Xiao et al., 2008).

The M-H curves for doped $LiCoO_2$ ($LiCo_{1-x}B_xO_2$ where x = 0.375 and 0.5) showed very weak hysteresis loops (Figure 4A) (Oz et al., 2016). Doping $LiCoO_2$ with gallium (Ga) revealed a weak Van Vleck paramagnetism above 100 K that increases with increasing Gallium content in all of the materials that were studied; magnetic transitions take place due to the $2Co^{3+} \rightarrow Co^{2+} + Co^{4+}$ equilibrium (all the species in low spin state) below 100 K (Gonzalo et al., 2010).

The magnetic properties of $Li_xNi_{2-x}O_2$, an active material used for cathodes, were studied. It was observed that the magnetic behavior of this material is correlated to the Li-Ni chemical composition range ordering that develops from short to long range. The boundaries between ordered domains generate an increased magnetic exchange bias, manifested as a change in the magnetization-field loop in the nanoscale regime of samples with consistent lengths ($0.54 < x < 0.66$) as shown in Figure 4B) (Barton et al., 2013). Also, for Li_xNiO_2 ($0.1 \leq x \leq 1$), it is observed that the magnetic susceptibility identifies the presence of spin-glass-like freezing at $T_f \sim 11$ K for the entire range of samples (all x). This suggests that macroscopic magnetism is not sensitive to x; however crystal structure and average oxidation state of the Ni in Li_xNiO_2 are altered with changing values of x (Mukai et al., 2009).

The $LiMPO_4$ (where M = Mn, Co, Ni) family of compounds comprised corner-sharing MO_6 octahedra of high-spin M^{2+} ions, which manifests as an antiferromagnetic ground state below $T_N \approx 30$ K (Ofer et al., 2012).

Lithium-iron phosphate ($LiFePO_4$) is a widely applied active material in cathode electrodes and exhibits paramagnetic behavior at temperatures above T_N with largest magnetic susceptibility in the b axis of 9.48×10^{-3} cm^3 mol^{-1} at room temperature (Zhou et al., 2019). Its magnetic behavior is dependent on temperature and shows a para-antiferromagnetic transition at T_N as observed in the Figure 4C) (Kim et al., 2019). In this structure, Fe ions are found in high spin configurations and have large magnetic moments (MMs), while the MMs of other ions are very small (Xiong et al., 2014). The MMs of the four Fe ions contained in the unit cell are parallel/antiparallel to the b-axis with the ordered moment (μ_{ord}) 4.19 μB at 2 K (Sugiyama et al., 2012).

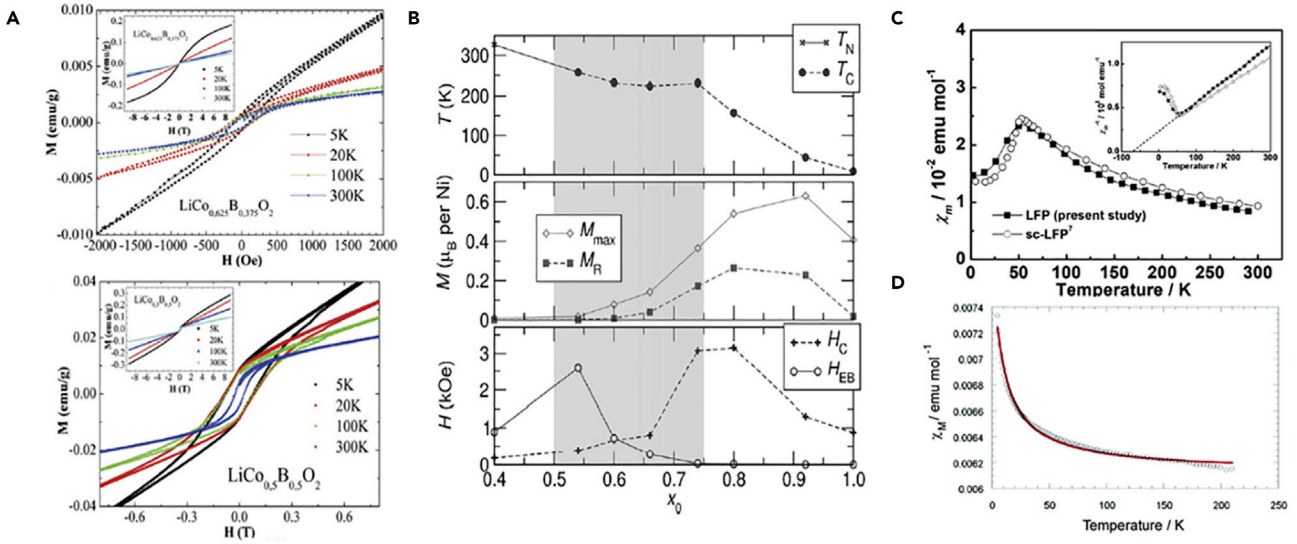

Figure 4. Magnetic characterization of different active materials

(A and B) (A) M-H curve of $LiCo_{1-x}B_xO_2$ samples where x = 0.375 (top) and x = 0.5 (bottom) (Oz et al., 2016), (B) Magnetic characteristics for $Li_xNi_{2-x}O_2$. The top section shows T_C and T_N, evident from features in the χ–T. M_{max} and M_R are shown in the middle section. M_{max} is the magnetization at T = 2 K and H = 5 T, whereas M_R is the remnant magnetization after the field is dropped to H = 0 T. The bottom section shows H_C and H_{EB}, as determined from the M–H loops. The shaded region indicates the composition range over which long-range chemical order is disrupted and magnetism changes nature (Barton et al., 2013).

(C) Temperature dependence of magnetic susceptibility and its reciprocal (inset) for $LiFePO_4$ (LFP) compared to the average magnetic susceptibility for single-crystal $LiFePO_4$ (sc-LFP), derived from the magnetic susceptibility along each crystal axis. The reciprocal plot for LFP was fitted with the Curie–Weiss law (dotted line, inset) (Kim et al., 2019).

(D) Molar susceptibility as a function of temperature for LiNiN (Stoeva et al., 2007).

The magnetic susceptibility of $LiFePO_4$ during charge and discharge behavior was evaluated; an oxidation from Fe(II) to Fe(III) was observed where the Li^+ ions are liberated with a reduction in the total MM of the non-stoichiometric Fe(II)/Fe(III) system due to a progressively quenched orbital magnetism (Gallien et al., 2014).

This active material was doped with transition metals such as Co, Mn, and La. This doping appears to degrade both the MM and the local moment on each dopant atom. As compared to the undoped sample, Fe atoms become nonmagnetic, resulting in decreased MMs (Xiao et al., 2016).

The evaluation of the magnetic properties of lithium-nickel/cobalt oxides and metal-substituted lithium-manganese spinel revealed electron spin resonance Ni^{3+} and Mn^{4+} and local short-range cation exchange interactions (Zhecheva et al., 2002). Also, LiNiN exhibits paramagnetic behavior; the molar susceptibility as a function of temperature is shown in Figure 4D (Stoeva et al., 2007).

Magnetic characterization was used to analyze delithiation of $Li_xCo_{0.8}Mn_{0.2}O_2$, and it was observed that chemical delithiation occurs only by oxidation of Mn^{3+} to Mn^{4+}, while cobalt remains in the trivalent state (Abuzeid et al., 2011). The evaluation of the delithiation process by magnetic characterization was also studied for $Li_yCo_{0.8}Ni_{0.1}Mn_{0.1}O_2$. Oxidation of Ni^{2+} and some Co^{3+} ions occurred at the beginning of the delithiation process (Labrini et al., 2016).

Lithium vanadium phosphate ($Li_3V_2(PO_4)_3$) was doped with Lanthanum (La) (Liu et al., 2015a) and neodymium (Nd) (Liu et al., 2015b), and its magnetic properties were evaluated. It was observed that the magnetic susceptibility decreases rapidly with increasing La content (Liu et al., 2015a) and increases with Nd content (except for x = 0.15) (Liu et al., 2015b). Also, the magnetic properties of $LiMg_{1-x}Zn_xVO_4$ spinels (where $0 \leq x \leq 1$) was evaluated. Magnetic susceptibility measurements confirmed Curie−Weiss behavior below 400 K with a μeff value of ~0.3 μB (Uyama et al., 2020). The magnetic properties of $Li_2Mn_2(MoO_4)_3$ indicated antiferromagnetic ordering among manganese ions at 1.4 K (Suleimanov et al., 2016).

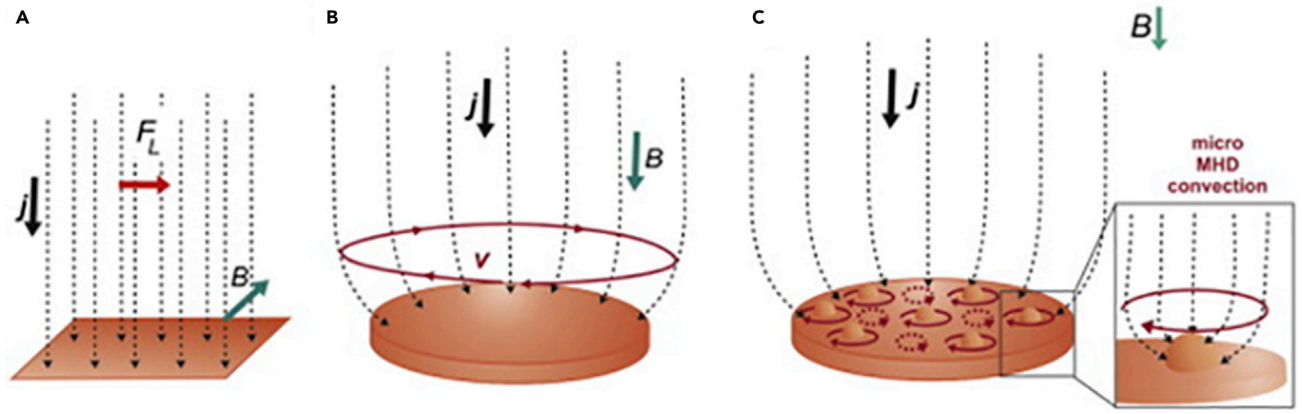

Figure 5. Different schemes of hydrodynamic flow at an electrode with different uniform magnetic fields applied

(A) Magnetic field applied parallel to the electrode surface (the primary MHD flow is parallel to the surface).

(B) Magnetic field applied perpendicular to the electrode surface (the primary MHD flow is a vortex around the rim).

(C) Magnetic field applied perpendicular to the electrode surface (secondary micro-MHD vortices arise around protuberances on the surface) (Monzon and Coey, 2014).

The magnetic characterization of active materials is thus essential in the context of lithium-ion batteries as some transition metals shows magnetic exchange strengths for redox processes which provides pathway to improve the charge-discharge behavior.

MHDs: mass transport

The interactions of charged particles within electric and MFs are governed by the MHD effect. This effect influences the dynamics of charged species present in an electrolyte due to a Lorentz force. This force is perpendicular to both electric and MFs. The Lorentz force causes moving charges to spiral, inducing convection of the electrolyte, which improves mass transfer and ion distribution.

When MFs are applied to an electrochemical cell, convection effect through the ions movement occur due to the MHD effect, as shown in Figure 5. The diffusion layer thickness is decreased, and mass transport is enhanced by the resulting flow from the interaction between the local current density and the fields. The threshold of the limiting current rises in the diffusion-controlled regime due to the electrolyte localized magnetic stirring (Monzon and Coey, 2014).

During the charge/discharge process, Li-ions present in the electrolyte shuttle from one electrode to another (intercalation/deintercalation processes), the essential working principle of the battery. Nonetheless, mass transport limitations are observed due to the thickness of both the electrodes and the separator. These thicknesses are defined by a compromise between operating voltage, ionic conduction, and energy density. For this reason, mass transport in the electrolyte is generally considered the one of the processes that limits the power density for LIBs (Hinds et al., 2001b). Mass transport is usually controlled by diffusion and migration (within micrometer-scale liquid layers and solids) in most battery systems, while convection has a negligible contribution (except on redox-flow batteries) (Personnettaz et al., 2019).

Upon cell discharge, Li ions migrate from the anode to the cathode as a result of an ohmic potential difference across the electrolyte. Simultaneously, anions flow in the opposite direction due to the aforementioned potential difference, resulting in a concentration difference across the electrolyte since the anions are unreactive at the electrodes. This concentration gradient creates an additional potential difference (diffusion potential), which is related to the diffusion flux of both the cations (Li^+) and the anions (present in electrolyte). The diffusion potential increases until the magnitude of the migration flux equals that of the diffusion flux. These magnitudes depend on the frictional forces that the charged species encounter in the electrolyte. For example, when an electrolyte contains anions with confined mobility, small differences in concentration are formed. Alternatively, if anions experience less frictional forces than Li^+, large concentration differences can be formed.

For this reason, MFs provide a suitable solution, since they are not dependent on chemical variations in the electrolyte, and they do not require the addition of new components that could compromise the batteries' performance. The effect that a MF has on mass transport is well documented (Chopart et al., 1991; Fahidy, 1983; Hinds et al., 2001b). The field causes convection in the electrolyte, the result of which is a narrowing of the diffusion layer. Several studies show that when an external MF interacts with an ionic current in an electrolyte, a flow within the solution is induced, which enhances the rate of the diffusional mass transfer (Aogaki et al., 1994). In this way, convection caused by the application of a MF increases the diffusion-limited current (Aaboubi et al., 1990; Aogaki et al., 1994; Fahidy, 1983; Tacken and Janssen, 1995).

The rate of transport may enhance dramatically by the presence of a MF; this is manifested experimentally by the improvements in the limiting current on the order of 100% for a range of systems (Mogi and Kamiko, 1996). The degree to which the current is enhanced depends on several properties of the electrolyte: concentration, solution viscosity, and the nature and concentration of the supporting electrolyte. Field-induced convection in the electrolyte is qualitatively equivalent to a gentle stirring (100 rpm of a rotating disk electrode), although the nature of this interaction is not well understood.

No magnetic ions need to be involved. As previously stated, it is well established that the primary magnetic force responsible for this effect is the Lorentz force (Hinds et al., 2001b). It has been demonstrated (Grant et al., 1999) that a tangential electric field close to the electrode surface is equivalent to the effect that a MF has on the limiting current. As mentioned previously, such an electric field may be created using a sweeping potential working electrode or by applying a MF parallel to the surface of the electrode.

Recently, the gradient forces have been claimed to generate similar effects on mass transport, and it is responsible for various observed effects (Leventis and Gao, 2002; O'Brien and Santhanam, 1997; Waskaas and Kharkats, 1999). Nevertheless, some studies claim that the effect of the gradient force created on mass transport should be negligible; it would need to be comparable in magnitude to this force to produce an observable effect (F_B/F_L ratio is of order 10^{-6} at room temperature (Hinds et al., 2001a)).

As mentioned previously, the field gradient force may become substantial in non-uniform MFs, at the macroscale of the entire cell or at the microscale at the surface of ferromagnetic electrodes (Grant et al., 1999; Yoshifumi et al., 2000). It has been reported (Mohanta and Fahidy, 1978) a significant enhancement in limiting current in non-uniform fields (average field strength one-tenth that of the uniform field strength required). Through the use of stirring bath, the field-induced enhancement in mass transport can be more easily achieved. However, once the force depends on the local current density, specific effects can be achieved when the MF or current density is strongly non-uniform, as in the vicinity of microelectrodes (Sueptitz et al., 2010).

Considering that the diffusion of the lithium ion into the electrode pores (porosity is necessary for the electrolyte solution to enter the electrode structure) is fundamental in the intercalation process, the magic-angle spinning, pulsed field gradient, stimulated-echo NMR was used to measure self-diffusion coefficients of the electrolyte species. The self-diffusion coefficient of Li^+ decreases with increasing carbon content and the tortuosity values of the electrodes contribute to specific interactions at the material/electrolyte interface on the lithium transport properties (Tambio et al., 2017).

MHDs: Electrode kinetics and morphology

There is still no directly observable evidence of the effect of an applied MF on electrode kinetics or of any influence in the rate of a heterogeneous electrochemical reaction (thermal energy and electrostatic potential energy are more substantial than magnetic energy). The electrode kinetics (Coey and Hinds, 2002), i.e. the effect of a MF on the kinetics of the electrode reaction, is a polemical and debatable topic. Several works assert that a MF has no effect on the kinetics of a battery (Cheng et al., 2017b; Chopart et al., 1991) or that it does not modify the charge-transfer parameters of the process (Devos et al., 2000).

Nevertheless, it has been observed adverse corrosion behavior of metals in contact with a flowing electrolyte in the presence of an applied MF (Kelly, 1977). The application of a MF can also enhance susceptibility to stress corrosion cracking, cause localized (pitting or crevice) corrosion, oxidize and reduce solution species, and, in the limit, electrochemically decompose the electrolyte.

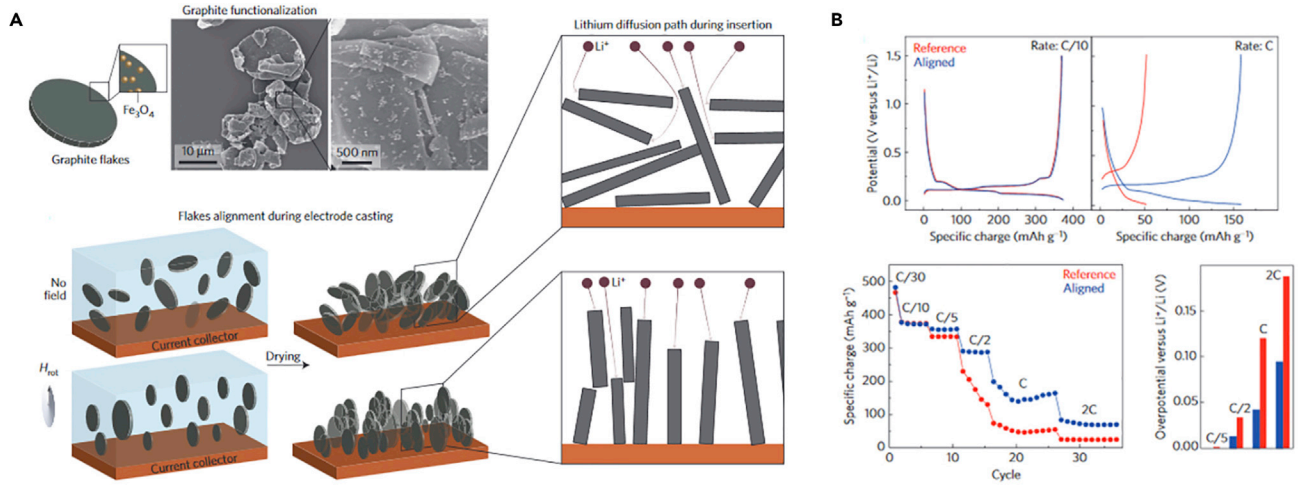

Figure 6. Electrode kinetics and morphology as a function of magnetic field

(A and B) (A) Schematic of the manufacture of the electrode under the influence of a magnetic field and (B) electrochemical performance of these electrodes (Billaud et al., 2016).

In anodic processes, shifts in the resting potential and enhanced corrosion of both magnetic and nonmagnetic electrodes have been observed (Lu et al., 2003; Rhen and Coey, 2007; Rhen et al., 2006). In this regime, an applied MF improves the flux of oxidant toward the surface, which is observed as anodic shifts in the rest potential (on the order of 100 mV). Any corroding electrode will experience anodic shifts due to microconvection from the Lorentz force, but there is an additional effect for a small ferromagnetic electrode, which creates a strong stay field in its vicinity (Yu et al., 2014). There is a local increase in pH, a decreased corrosion current, and a cathodic shift of the rest potential (Sueptitz et al., 2010, 2011).

MFs have been found to influence several anodic process, such as polymerization (Kołodziejczyk et al., 2018), oxidation at electroactive self-assembled monolayers, corrosion control and electropolishing, improvement of surface finish of electropolished, biocompatible metallic alloys. They have even been found to be enhanced by more than 25% of the performance of nickel metal hydride batteries (O'Brien, 2019).

The MF effects that have been observed on the morphology of electrodeposited materials are frequently related to those of mass transport. Owing to field-induced convection, the application of a MF during electrodeposition can change the pattern structure formation of two-dimensional fractal electrodeposits (Coey et al., 1999; Mogi and Kamiko, 1996) and smoothen the surface of electroplated films (Kudo and Mogi, 1995). A hydrothermal technique involving a pulsed MF of high intensity paired with an aging technique has successfully synthesized nanocrystalline Co_3O_4. Processing with a pulsed MF produces a more compact and smooth surface composed of Co_3O_4 microspheres containing numerous nanograins (Rahman et al., 2009).

During electrode preparation, the application of MFs improves the orientation of graphite particles (aligned, out-of-plane architecture) in LIBs (Billaud et al., 2016), lithium polysulfide and magnetic nanoparticles in a lithium metal-polysulfide semi-liquid battery (Li et al., 2015) and $LiCoO_2$ electrodes (Sander et al., 2016a). For the graphite anodes, the lower tortuosity allows us to improve mass transport and leads to a specific capacity (~100 $mAh.g^{-1}$) up to three times higher than that of non-aligned electrodes at the same rate (1C) (Billaud et al., 2016), as shown in Figure 6.

For cathodes, directional pores yield faster charge transport kinetics and enable electrodes with more than threefold higher areal capacity due to the reduction of the tortuosity (Sander et al., 2016a).

Regarding the later approach, the conductivity in the electrode simply improves if there is less tortuosity (Sander et al., 2016a). These approaches are achieved with dispersed magnetic material in the electrodes aligned with an external MF, which creates an anisotropy. In the case of lithium cobalt oxide ($LiCoO_2$)

electrodes, the usable capacity of the electrodes increased by a factor of three, the areal capacities were measured to be over 8 $mAh \cdot cm^{-2}$ (over two times than the ones present in conventional Li-ion electrodes) and the discharge profiles are in line with the drive cycles of EVs.

Also, the MF of 5 kOe was used to align and pattern multiwall carbon nanotube channels in a polystyrene matrix for electrodes in LIBs, resulting in an increase of the electrochemical behavior (charge-discharge values) and rate capability (Tripathi et al., 2017).

Lithium metal is the most attractive anode for LIBs, and it is one of the most studied in the scientific community. This material possesses a low density, a high specific capacity, and a favorable redox potential. However, safety and cycling stability are jeopardized by the formation of lithium dendrites, which are created due to non-uniform Li^+ concentration on the electrode surface (Cheng et al., 2018).

In order to improve the performance and safety of Li metal anodes, different strategies have been applied to inhibit and eliminate the growth of dendrites, which could be classified into two main groups: internal and external strategies (Dash and King, 1972). The former modifies or optimizes the components inside the cells, which could effectively suppress dendrite formation, but the change of the cell environment could lead to cell instability. The use of additives and the modification of the electrode represent two avenues that could lead to cell instability, specific examples of which include electrolyte optimization, artificial SEI design, and synthesis of 3D current collector (Cheng et al., 2017b).

Further, metal electroplating process is also a concern, since the quality of the lithium deposit is of primary interest. Numerous studies in the literature regarding the MF effect on the deposited surface pattern report contradictory observations, since morphological characteristics of the deposited crystal structure cannot be definitively attributed to the imposed magnetic flux density. Nevertheless, there is substantial evidence to support the beneficial effects of an applied, uniform MF on surface evenness and hardness (Dash and King, 1972; Mohanta and Fahidy, 1972) under certain conditions.

Electrochemical deposition under MF (ED-MF) is extensively used for the preparation of a variety of metals, such as Cu (Miura et al., 2017; Mühlenhoff et al., 2013), Co (Devos et al., 2000), and Ni-Mo (Aaboubi et al., 2015) due to the advantages of high energy density, ease of control, noncontact energy transfer, and high selectivity. The MHD effect (Monzon and Coey, 2014) causes a uniform flux of Li^+, a suppression of Li dendrites, and the formation of dense deposits (Cheng et al., 2017b; Rhen et al., 2006; Shi et al., 2017; Sueptitz et al., 2010). As an example, the external strategy has been applied, which is less aggressive and more efficient, as an alternative to the internal changes mentioned above (Figure 7).

For example, the MHD effect (Shen et al., 2019) has been used to effectively promote mass transfer and uniform distribution of Li^+, to suppress dendrite growth, and to obtain uniform and compact lithium deposits. By using an external MF to redistribute the concentration of Li^+ on the anode surface, uniform lithium deposition could be achieved. The researchers successfully showed that lithium metal anodes within a MF exhibit excellent cycling and rate performance in a symmetrical battery. In addition, full cells utilizing lithium metal as anodes and commercial $LiFePO_4$ as cathodes show improved performance within the MF.

The applied MF can significantly refine grain size, obtain uniform structure, and affect texture and dendrite growth direction (Melot et al., 2011; Priest and Forbes, 2007). Essentially, since the plating of lithium anodes is an ED, the MHD effect may also benefit the electrode reactions of Li metal batteries. The MHD effect has significant influence on morphology, structure, and properties of deposition layer for copper metal. Moreover, also benefits the performance of the batteries, which exhibited much-improved electrochemical performance of charge-discharge values, the coulombic efficiency (CE) and enhancing the cycling stability significantly (Miura et al., 2017; Tang et al., 2017).

In J. K. Koper's study (Koper, 2018), applying an MF shortened the dendrites formed in the silver and shrank the crystal dimensions during silver deposition with the external field interacting perpendicularly to the sample surface. The dendrites are promoted by the pre-modified surface, by anodic oxidation, although the applied field avoids the expansion of the dendrites and changes the nucleation stage during the deposition process. The author also reported differences when switching the field, modifying the morphology of the deposited material, the particles of the silver that are deposited become thinner or thicker, depending on the sense of the MF. Also, it

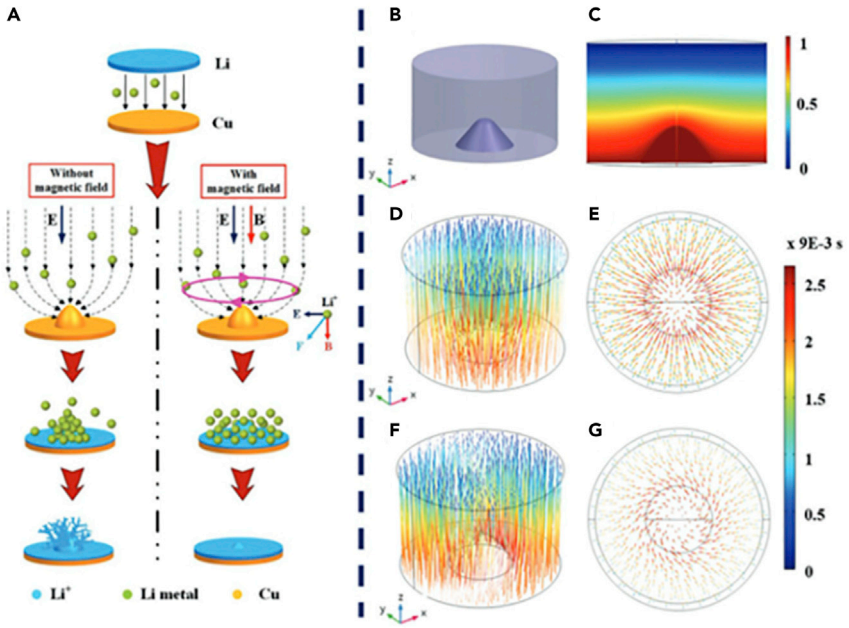

Figure 7. Electrochemical deposition under magnetic field

(A) Schematic illustration of the effects of a magnetic field on Li^+ deposition.

(B) The skeleton diagram of a small feature on surface of the anode.

(C) The potential distribution near the feature. The scale to the right is the ratio of relative voltage.

(D–G) Simulation results of the different trajectories of Li^+ during deposition without (D) and (E) or within (F) and (G) a magnetic field. The scale to the right represents the timeline (Shen et al., 2019).

was evaluated in situ by magnetic resonance imaging (MRI), in lithium cells that presents symmetry, the mechanism under the dendrites grow, always searching the same conditions of work, these evaluations were made on the electrodes and the electrolyte. These results gave an insight on how the depletion of the electrolyte and the starting point at which the dendrite start growing are related in a strong way, all this happening at the surface of the electrode; besides the MRI results exhibited as well, rates of charge higher than usual. The presented MRI approach allows the correlation of the nature of the process happening at the electrode, together with the electrolyte and the presented rate (Chang et al., 2015).

Also, MRI technique allows for the mapping of the fields during the charge and discharge processes; this mapping shows that the charging state, together with the damages happening in a sustainable way, alter the distribution of the fields (Mohammadi et al., 2019).

The solvation behavior was also studied by NMR technique, in common electrolyte solutions (such as $LiPF_6$, and or LiBF4) dissolved in ethylene carbonate and dimethyl carbonate. The ion aggregations (in both electrolytes) are more favorable by a low polarity in the solvent (as the DMC content increases), but much more in the $LiBF_4$, as observed through the decreasing of ^{11}B relaxation time and Li^+, anion diffusion coefficients. During the ion association in the $LiPF_6$ electrolyte, the concentration of salt is not that significant, and this was proven by changing the DMC concentration and observing that the ratio of the F^- and Li^+ mobility (1.0 M and 0.01 M) is equal. The opposite situation was observed in the $LiBF_4$ system, where the aggregation of ions was much higher (Peng et al., 2018).

Yet-Ming Chiang et al. (Li et al., 2019) formulated a method, by alignment with applied MF, to use in anodes and cathodes materials base on powder, which can be processesed by water-based methods, to reduce the tortuosity at the electrodes, as well as increase the its capacity and increase its thickness as shown in Figure 8.

This method might show interesting fast charging results if it is applied to the negative electrodes, since it allows us to incorporate additives to enhance the properties, such as mechanical and conductivity. The development of this method is still in diapers, but it might improve the energy density and the

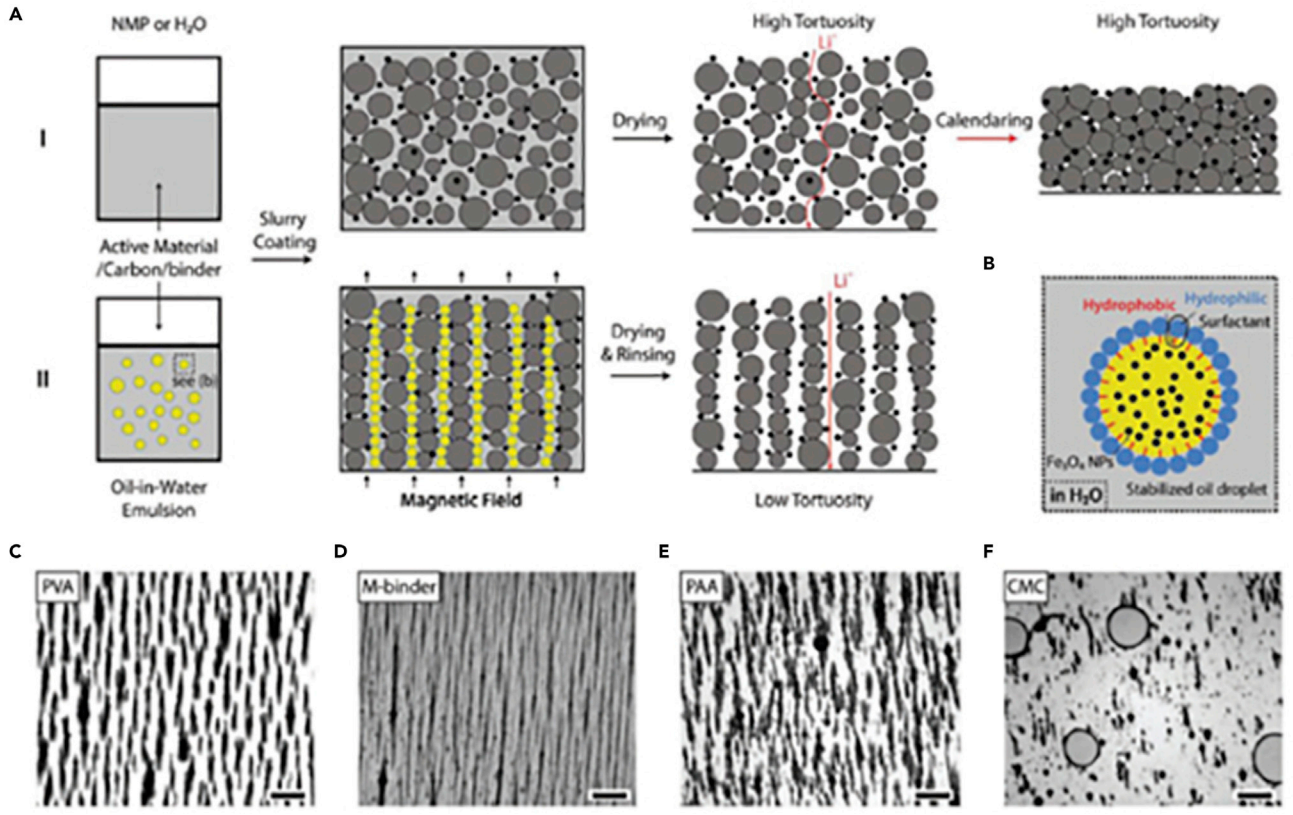

Figure 8. – Demonstration of how to prepare low-tortuosity electrodes

(A) Schema of the conventional methods (I) and the proposed one to decrease the tortuosity. The active material of carbon black nanoparticles (NPs) and stabilized magnetite-NP-containing oil droplets are represented by gray, black, and yellow spheres, respectively. The aligned porosity is created by the alignment of the oil droplets by the external field and then dried and removed.

(B) Drawing of the magnetite-NP with the oil droplets. The surfactant has stabilized the oil droplets.

(C–F) Images of aligned droplets in 1.5 wt.% PVA, by the external field, taken by optical microscopy. Different components of (C), M-binder (D), PAA (E), and CMC (F) in one drop (50 μL) of oil-in-water emulsion. The scale bars represent 100 μm in (C, E, and F), and 200 μm in (D). In (C–F) the dark phase is the oil droplets and the light phase is the aqueous solution including the surfactant (Li et al., 2019).

fast-charging process, by thickening the electrodes. Other approaches have been presented to improve the capacity of the batteries with thicker electrodes, by creating anisotropy and low tortuosity (Sander et al., 2016b). These two processes have lower cost, scalable to large areas, and are faster to perform. In the former, the researchers produced faster transport in the electrodes by creating anisotropic pores aligned with the charge transport direction, allowing thicker electrodes to have faster and more efficient transport.

It has proven that the homogeneity of the metal deposition may improve significantly by a good configuration of the Lorentz forces with specific conditions, for example with a higher gradient of the field, although the MHD effect is the key to obtain a homogeneous current density distribution to get an electrochemically deposited metal layer (Kudo and Mogi, 1995). According to their studies, inhomogeneities in the deposited layer indicate an inhomogeneous current distribution.

The Lorentz force's impact on the performance of an LIB with $LiFePO_4$ electrodes enhanced with γ-Fe_2O_3 was studied, where through the Lorentz force theory, an improvement in specific capacity was observed at high current rates in which the incorporation of γ-Fe_2O_3 at the cathode raise the power density and life cycle of LIBs, strategically (Cheng et al., 2017a).

LIBs using $MnFe_2O_4$ and γ-Fe_2O_3 as electrodes were fabricated, where they show a controllable magnetization, which was controlled electrically, over a magnitude of 10%, in between the values of 1.5 V and -3′.0 V.

This change of the magnetization saturation has been explained by the mechanism of modulation caused by exchange coupling and magnetic ion migration (Wei et al., 2017a).

The performance of the batteries can be improved by adding other ways to control the conduction of the materials, as for example magnetic semiconductors, which so far are an innovative method. These new actors in electronic applications are under exploration for application in batteries and energy storage since they are semiconductors materials that present ferromagnetism (in which the spin can be managed) and semiconductors properties (controlling the charge carriers). This phenomenon is present in semiconductors of Mn-doped III-Vs, (for example (In,Mn)As and (Ga,Mn)As), where it is possible to induce and manipulate the modification of carrier concentration by ferromagnetism (Ohno et al., 1992, 1996).

In this kind of semiconductors, an effective MF can be induced by current through a spin-orbit interaction, which makes possible to switch the magnetization from one stable state to another one with no field. This effect is referred as an electric-field switching of magnetization (change of the magnetic anisotropy by changing the carrier concentration).

An interesting approach to the design of smart battery architecture was developed through a magnetic-manipulated electrode exploring magnetic Fe_3O_4 particles as binder, leading to non-fatigue performance (Liu et al., 2015c).

In addition to the electrodes, the solid electrolyte material of glass ceramics based on lithium aluminum phosphate with different Fe_2O_3 was developed for LIBs in which this material has magnetic properties (Abo-Mosallam and Farag, 2020).

For poly(ethylene oxide) block-based solid polymer electrolytes, the membrane has been optimized through the alignment of self-assembled structures by MFs. Also, it is observed that at the membrane, the field magnitude and the temperature alter the conductivity of the ions. For example, when applying a field of 6 T, there is a increase of one order of magnitude in the conductivity when compared to the non-aligned case (Majewski et al., 2010).

Moreover, poly (ethylene oxide) (PEO)-based solid polymer electrolytes with functionalized sepiolite (KFSEP) nanowires have been developed for LiBs. The magnetic alignment of the nanowires provides a fast-moving channel for lithium ions (Han et al., 2021).

Manipulation of LIB by an applied MF

An external field is a non-invasive technique, which is an important consideration when evaluating the SEI during the charging and discharging cycles.

It is essential to understand how the efficiency, performance and life cycle behaves with the Li-ion battery calendar lifetime, since aging is the reason of the decrease or total loss of their performance (in terms of energy, power, capacity, and thermal) (Panchal et al., 2017a, 2017b). The physical and chemical changes, which are irreversible in these devices (e.g. SEI modifications, cracks in the electrodes, internal resistance, electrolyte decomposition) are the reason of the degradation of the batteries performance (Singh et al., 2018).

At the beginning of the LIBs charge/discharge cycles, the electrolyte is electrochemically reduced at the surface of the anode. From this reduction, an insoluble passivating film is created on the anode surface – SEI (Wang et al., 2019b). The formed film is a critical component of LIBs since it prevents additional parasitic electrolyte decomposition, and it contributes to the stabilization of the battery operation and capacity (Verma et al., 2010). Consequently, the charging cycles process of the battery, at its beginnings, depends essentially on the creation of the layer of the SEI (Miura et al., 2017), since the electrolyte is protected by the SEI film, avoiding an increased exhaustion and the anode from corrosion since vigorous reactions arise between electrolyte material and anode material at the initial battery charging processes (Miura et al., 2017). Some experimental studies, such as that performed by Ganguly et al. (Ganguly et al., 2020), demonstrate how an external field over a α-Fe_2O_3/NC anode battery enhances the first and second cycle CE from 70% (without applied MF) to 73.5% (with field), on the first cycle. Moreover, the increasing of the specific capacity from 1500 to 1700 mAh/g and from 1100 to 1300 mAh/g for a density of current of 50 mA/g, on first and

second discharge cycle, respectively, was observed. The reason for this enhancement is associated with the lower loss of lithium ions for SEI formation, superior lithium-ion transportation, and reduction in the electrochemical overpotentials when the battery is subjected to a MF.

It was proven that the process of the cycling, i.e. charging and discharging, can control the magnetization of the LIB, when the electrodes are designed with nanomaterials (Zhang et al., 2016). With the control of the lithiation and the delithiation processes of α-Fe_2O_3-based electrodes at the nanometer scale, the management of magnetism, in a reversible way, was achieved three orders of magnitude higher. This work provides an exciting prospect for the manipulation of the magnetic properties, reversibly, in LIBs where its behavior can be magnetically controlled on-demand. In addition, the MF can operate as a battery switch through the incorporation of a magnetic control component in its structure. It was observed that this component design allows switching between an insulating condition and a conductive one, for more than 500 cycles, since it is reversible while maintaining superior cycle stability (Zhang et al., 2020). The superior performance, electrochemically, in a large potential range, can be preserve in batteries with this built-in component at normal conditions.

The application of a MF during LIBs operation represents the combination of two fields, magnetism and electrochemistry, the magnetization variation allowing us to improve the electrochemical response. The effect of the MF application on the electrochemical processes is mainly related to: (a) on suppression of the lithium dendrite growth, (b) orientation of the active materials during electrode preparation for reducing tortuosity and (c) inhibition of the SEI between the electrode and the electrolyte.

In addition, the external MF allows us to improve the charge/discharge behavior of LIBs, by tuning the lithiation/delithiation process.

Continuous developments are nevertheless needed in this field to improve the use of electrochemically active molecules based on magnetically responsive elements, as well as to optimize the effect of the applied MF in the different processes. Finally, it is also necessary to develop compact systems to be incorporated into practical applications to apply MFs during the electrochemical behavior of the batteries.

FINAL CONSIDERATIONS AND FUTURE TRENDS

LIBs have been studied over the last years, being today the most used energy storage system. Their functionality under an applied MF has been studied since the 80's, showing that LIB performance can be improved (a) by eliminating lithium dendrite growth, (b) by the orientation of the active materials during electrode preparation to reduce tortuosity, and (c) by preventing the SEI, based on the paramagnetic character of lithium ions, allowing to reduce the concentration of active materials in the electrodes with the applied MF. All those issues represent important factors contributing to the stabilization and improvement of the operation and capacity of the battery. Magnetic body force effects in the conductivity are assumed to be responsible for this improvement. The MHD effect is responsible for the ion movement originated by the electro MF (Lorentz force). This effect efficiently fosters the transfer of mass and a distribution of the lithium ions uniformly in the electrodes resulting in an inhibition of dendrite growth. The magnetic susceptibility of the active material of LIBs is an important property to explore once the magnetic properties of the transition metal redox processes begin to be correlated to the electrical control (voltage) of LIBs, influencing battery performance. Magnetic manipulation and tuning of the magnetic susceptibility of active materials, by a MF, will control the electrolyte properties, mass transportation, electrode kinetics, and deposit morphology. These concepts can solve some existing drawbacks,not only in LIBs but also in electrochemical batteries in general. Also, allied to powerful tools as magnetic characterization and simulation systems, promising new concepts, systems and materials of LIBs will raise.

ACKNOWLEDGMENTS

Work supported by the Portuguese Foundation for Science and Technology (FCT): projects UID/FIS/04650/2020, UID/CTM/50025/2020, UID/QUI/50006/2020, PTDC/FIS-MAC/28157/2017, Grant SFRH/BPD/112547/2015 (C.M.C.), and Investigator FCT Contract CEECIND/00833/2017 (R.G.) and 2020.04028.CEECIND (C.M.C.), as well POCH and European Union. Financial support from the Basque Government Industry and Education Departments under the ELKARTEK and PIBA (PIBA-2018-06) programs is also acknowledged.

AUTHOR CONTRIBUTIONS

Conceptualization, C.M.C. and S.L.-M; writing - original draft, C.M.C., K.J.M., R.G., C.A., and S.L.-M; writing - review & editing, C.M.C., K.J.M., R.G., C.A., and S.L.-M; Funding acquisition, S.L.-M.

REFERENCES

Aaboubi, O., Ali Omar, A.Y., Franczak, A., and Msellak, K. (2015). Investigation of the electrodeposition kinetics of Ni–Mo alloys in the presence of magnetic field. J. Electroanal. Chem. *737*, 226–234. https://doi.org/10.1016/j.jelechem.2014.10.014.

Aaboubi, O., Chopart, J.P., Douglade, J., Olivier, A., Gabrielli, C., and Tribollet, B. (1990). Magnetic field effects on mass transport. J. Electrochem. Soc. *137*, 1796–1804. https://doi.org/10.1149/1.2086807.

Abo-Mosallam, H.A., and Farag, M.M. (2020). Preparation, crystallization features and electro-magnetic properties of phosphate based glass-ceramics as solid electrolyte for lithium-ion batteries. J. Aust. Ceram. Soc. *56*, 353–361. https://doi.org/10.1007/s41779-019-00406-7.

Abuzeid, H.A.M., Hashem, A.M.A., Abdel-Ghany, A.E., Eid, A.E., Mauger, A., Groult, H., and Julien, C.M. (2011). De-intercalation of LixCo0.8Mn0.2O2: a magnetic approach. J. Power Sourc. *196*, 6440–6448. https://doi.org/10.1016/j.jpowsour.2011.03.054.

Aogaki, R., Negishi, T., Yamato, M., Ito, E., and Mogi, I. (1994). Hysteresis effect of magnetic field on electron transfer processes in electrochemical reaction. Phys. B Condens. Matt. *201*, 611–615. https://doi.org/10.1016/0921-4526(94)91172-X.

Barton, P.T., Premchand, Y.D., Chater, P.A., Seshadri, R., and Rosseinsky, M.J. (2013). Chemical inhomogeneity, short-range order, and magnetism in the LiNiO2-NiO solid solution. Chem. A Eur. J. *19*, 14521–14531. https://doi.org/10.1002/chem.201301451.

Billaud, J., Bouville, F., Magrini, T., Villevieille, C., and Studart, A.R. (2016). Magnetically aligned graphite electrodes for high-rate performance Li-ion batteries. Nat. Energy *1*, 16097. https://doi.org/10.1038/nenergy.2016.97. https://www.nature.com/articles/nenergy201697#supplementary-information.

Chang, H.J., Ilott, A.J., Trease, N.M., Mohammadi, M., Jerschow, A., and Grey, C.P. (2015). Correlating Microstructural lithium metal growth with electrolyte salt depletion in lithium batteries using 7Li MRI. J. Am. Chem. Soc. *137*, 15209–15216. https://doi.org/10.1021/jacs.5b09385.

Cheng, H.-M., Wang, F.-M., and Chu, J.P. (2017a). Effect of Lorentz force on the electrochemical performance of lithium-ion batteries. Electrochem. Commun. *76*, 63–66. https://doi.org/10.1016/j.elecom.2017.01.022.

Cheng, Q., Wei, L., Liu, Z., Ni, N., Sang, Z., Zhu, B., Xu, W., Chen, M., Miao, Y., Chen, L.-Q., et al. (2018). Operando and three-dimensional visualization of anion depletion and lithium growth by stimulated Raman scattering microscopy. Nat. Commun. *9*, 2942. https://doi.org/10.1038/s41467-018-05289-z.

Cheng, X.-B., Zhang, R., Zhao, C.-Z., and Zhang, Q. (2017b). Toward safe lithium metal anode in rechargeable batteries: a review. Chem. Rev. *117*, 10403–10473. https://doi.org/10.1021/acs.chemrev.7b00115.

Chernova, N.A., Nolis, G.M., Omenya, F.O., Zhou, H., Li, Z., and Whittingham, M.S. (2011). What can we learn about battery materials from their magnetic properties? J. Mater. Chem. *21*, 9865–9875. https://doi.org/10.1039/c1jm00024a.

Chien, C. (2013). The Hall Effect and its Applications (Springer US).

Chopart, J.P., Douglade, J., Fricoteaux, P., and Olivier, A. (1991). Electrodeposition and electrodissolution of copper with a magnetic field: dynamic and stationary investigations. Electrochim. Acta *36*, 459–463. https://doi.org/10.1016/0013-4686(91)85128-T.

Coey, J.M.D., Hinds, G., and Lyons, M.E.G. (1999). Magnetic-field effects on fractal electrodeposits. Europhysics Lett. *47*, 267–272. https://doi.org/10.1209/epl/i1999-00382-3.

Coey, M., and Hinds, G. (2002). Magnetoelectrolysis - the effect of magnetic fields in electrochemistry. 5th International Pamir Conference at Ramatuelle, France.

Coquil, G., Fullenwarth, J., Grinbom, G., Sougrati, M.T., Stievano, L., Zitoun, D., and Monconduit, L. (2017). FeSi4P4: a novel negative electrode with atypical electrochemical mechanism for Li and Na-ion batteries. J. Power Sourc. *372*, 196–203. https://doi.org/10.1016/j.jpowsour.2017.10.069.

Costa, C.M., Lee, Y.-H., Kim, J.-H., Lee, S.-Y., and Lanceros-Méndez, S. (2019). Recent advances on separator membranes for lithium-ion battery applications: from porous membranes to solid electrolytes. Energy Storage Mater. *22*, 346–375. https://doi.org/10.1016/j.ensm.2019.07.024.

Costa, C.M., Silva, M.M., and Lanceros-Mendez, S. (2013). Battery separators based on vinylidene fluoride (VDF) polymers and copolymers for lithium ion battery applications. RSC Adv. *3*, 11404–11417. https://doi.org/10.1039/c3ra40732b.

Dash, J., and King, W.W. (1972). Electrothinning and electrodeposition of metals in magnetic fields. J. Electrochem. Soc. *119*, 51. https://doi.org/10.1149/1.2404131.

Devos, O., Aaboubi, O., Chopart, J.-P., Olivier, A., Gabrielli, C., and Tribollet, B. (2000). Is there a magnetic field effect on electrochemical kinetics? J. Phys. Chem. A *104*, 1544–1548. https://doi.org/10.1021/jp993696v.

Duan, L., Gao, F., Wang, L., Jin, S., and Wu, H. (2013). Hydrothermal synthesis and characterization of MnCo2O4 in the low-temperature hydrothermal process: their magnetism and electrochemical properties. J. Adv. Ceramics *2*, 266–273. https://doi.org/10.1007/s40145-013-0070-0.

Eom, T.H., Xiao, Y., Han, J.I., and Zhang, F.C. (2017). Electrical structure, magnetic polaron and lithium ion dynamics in four mixed-metal oxide multiple-phase electrode cathode material for Li ion batteries from density functional theory study. Comput. Mater. Sci. *132*, 92–103. https://doi.org/10.1016/j.commatsci.2017.02.025.

Fahidy, T.Z. (1983). Magnetoelectrolysis. J. Appl. Electrochem. *13*, 553–563. https://doi.org/10.1007/BF00617811.

Gallien, T., Krenn, H., Fischer, R., and Wegleiter, H. (2014). Magnetism vs. LiFePO4 battery's state of charge: A route to a novel sensor concept, 29th Conference on Precision Electromagnetic Measurements (CPEM 2014), pp. 648–649.

Ganguly, D., V.S.,A.P., Ghosh, A., and Ramaprabhu, S. (2020). Magnetic field assisted high capacity durable Li-ion battery using magnetic α-Fe2O3 nanoparticles decorated expired drug derived N-doped carbon anode. Sci. Rep. *10*, 9945. https://doi.org/10.1038/s41598-020-67042-1.

Gonzalo, E.C., Morán, E., Parada, C., and Ehrenberg, H. (2010). Microwave-assisted synthesis of LiCoO2 and LiCo1−xGaxO2: Structural features, magnetism and electrochemical characterization. Mater. Chem. Phys. *121*, 484–488. https://doi.org/10.1016/j.matchemphys.2010.02.011.

Grant, K.M., Hemmert, J.W., and White, H.S. (1999). Magnetic focusing of redox molecules at ferromagnetic microelectrodes. Electrochem. Commun. *1*, 319–323. https://doi.org/10.1016/S1388-2481(99)00065-X.

Guo, J., Chen, L., Zhang, X., Zhou, X., Wang, G., and Jiang, B. (2013). Tungsten doping magnetic iron oxide and their enhanced lithium ion storage properties. Mater. Lett. *106*, 304–307. https://doi.org/10.1016/j.matlet.2013.05.046.

Guo, X., Liang, X., Zhou, X., Hu, S., He, W., and Guo, G. (2020). Structural, magnetic, and electrochemical properties of hierarchical microspindle-like Fe2−xMnxO3 composites from thermal decomposition of oxalates. J. Mater. Sci. Mater. Electron. *31*, 3986–3995. https://doi.org/10.1007/s10854-020-02946-2.

Han, L., Wang, J., Mu, X., Wu, T., Liao, C., Wu, N., Xing, W., Song, L., Kan, Y., and Hu, Y. (2021). Controllable magnetic field aligned sepiolite nanowires for high ionic conductivity and high safety PEO solid polymer electrolytes. J. Colloid Interf. Sci. *585*, 596–604. https://doi.org/10.1016/j.jcis.2020.10.039.

Hayner, C.M., Zhao, X., and Kung, H.H. (2012). Materials for rechargeable lithium-ion batteries. Annu. Rev. Chem. Biomol. Eng. *3*, 445–471. https://doi.org/10.1146/annurev-chembioeng-062011-081024.

Hinds, G., Coey, J.M.D., and Lyons, M.E.G. (2001a). Influence of magnetic forces on electrochemical mass transport. Electrochem.

Commun. *3*, 215–218. https://doi.org/10.1016/S1388-2481(01)00136-9.

Hinds, G., Spada, F.E., Coey, J.M.D., Ní Mhíocháin, T.R., and Lyons, M.E.G. (2001b). Magnetic field effects on copper electrolysis. J. Phys. Chem. B *105*, 9487–9502. https://doi.org/10.1021/jp010581u.

Huang, K.-P., Fey, G.T.-K., Lin, Y.-C., Wu, P.-J., Chang, J.-K., and Kao, H.-M. (2017). Magnetic impurity effects on self-discharge capacity, cycle performance, and rate capability of LiFePO4/C composites. J. Solid State Electrochem. *21*, 1767–1775. https://doi.org/10.1007/s10008-017-3527-1.

Huyan, Y., Wang, J., Chen, J., Zhang, Q., and Zhang, B. (2019). Magnetic tubular carbon nanofibers as anode electrodes for high-performance lithium-ion batteries. Int. J. Energy Res. *43*, 8242–8256. https://doi.org/10.1002/er.4821.

Julien, C., Mauger, A., Zaghib, K., and Gendron, F. (2007). 2nd International Conference on Physics of Solid State Ionics at: Yokohama, Japan. Abstr., p. 27.

Kelly, E.J. (1977). Magnetic field effects on electrochemical reactions occurring at metal/flowing-electrolyte interfaces. J. Electrochem. Soc. *124*, 987–994. https://doi.org/10.1149/1.2133514.

Kim, C., Yang, Y., Ha, D., Kim, D.H., and Kim, H. (2019). Crystal alignment of a LiFePO4 cathode material for lithium ion batteries using its magnetic properties. RSC Adv. *9*, 31936–31942. https://doi.org/10.1039/C9RA05284D.

Kołodziejczyk, K., Miękoś, E., Zieliński, M., Jaksender, M., Szczukocki, D., Czarny, K., and Krawczyk, B. (2018). Influence of constant magnetic field on electrodeposition of metals, alloys, conductive polymers, and organic reactions. J. Solid State Electrochem. *22*, 1629–1647. https://doi.org/10.1007/s10008-017-3875-x.

Koper, J. (2018). The influence of magnetohydrodynamic power on the deposition of silver dendrites on the titanium surface after anodic oxidation. Int. J. Electrochem. Sci. *13*, 699–707. https://doi.org/10.20964/2018.01.89.

Kudo, S., and Mogi, I. (1995). Effect of a high magneic field on the electrodeposition of Tl2O3 films. Denki Kagaku *63*, 238–240. https://doi.org/10.5796/kogyobutsurikagaku.63.238.

Labrini, M., Scheiba, F., Almaggoussi, A., Larzek, M., Braga, M.H., Ehrenberg, H., and Saadoune, I. (2016). Delithiated LiyCo0.8Ni0.1Mn0.1O2 cathode materials for lithium-ion batteries: Structural, magnetic and electrochemical studies. Solid State Ionics *289*, 207–213. https://doi.org/10.1016/j.ssi.2016.03.017.

Leventis, N., and Gao, X. (2002). Nd−Fe−B permanent magnet electrodes. theoretical evaluation and experimental demonstration of the paramagnetic body forces. J. Am. Chem. Soc. *124*, 1079–1088. https://doi.org/10.1021/ja0121991.

Li, L., Erb, R.M., Wang, J., Wang, J., and Chiang, Y.-M. (2019). Fabrication of low-tortuosity ultrahigh-area-capacity battery electrodes through magnetic alignment of emulsion-based slurries. Adv. Energy Mater. *9*, 1802472. https://doi.org/10.1002/aenm.201802472.

Li, W., Liang, Z., Lu, Z., Tao, X., Liu, K., Yao, H., and Cui, Y. (2015). Magnetic field-controlled lithium polysulfide semiliquid battery with ferrofluidic properties. Nano Lett. *15*, 7394–7399. https://doi.org/10.1021/acs.nanolett.5b02818.

Lin, X., Lv, X., Wang, L., Zhang, F., and Duan, L. (2013). Preparation and characterization of MnFe2O4 in the solvothermal process: their magnetism and electrochemical properties. Mater. Res. Bull. *48*, 2511–2516. https://doi.org/10.1016/j.materresbull.2013.03.010.

Liu, L., Lei, X., Tang, H., Zeng, R., Chen, Y., and Zhang, H. (2015a). Influences of La doping on magnetic and electrochemical properties of Li3V2(PO4)3/C cathode materials for lithium-ion batteries. Electrochim. Acta *151*, 378–385. https://doi.org/10.1016/j.electacta.2014.11.052.

Liu, L., Qiu, Y., Mai, Y., Wu, Q., and Zhang, H. (2015b). Influences of neodymium doping on magnetic and electrochemical properties of Li3V2(PO4)3/C synthesized via a sol–gel method. J. Power Sourc. *295*, 246–253. https://doi.org/10.1016/j.jpowsour.2015.06.121.

Liu, X., Li, D., Bai, S., and Zhou, H. (2015c). Promotional recyclable Li-ion batteries by a magnetic binder with anti-vibration and non-fatigue performance. J. Mater. Chem. A *3*, 15403–15407. https://doi.org/10.1039/C5TA04342E.

Lu, Z., Huang, D., Yang, W., and Congleton, J. (2003). Effects of an applied magnetic field on the dissolution and passivation of iron in sulphuric acid. Corrosion Sci. *45*, 2233–2249. https://doi.org/10.1016/S0010-938X(03)00045-3.

Majewski, P.W., Gopinadhan, M., Jang, W.-S., Lutkenhaus, J.L., and Osuji, C.O. (2010). Anisotropic ionic conductivity in block copolymer membranes by magnetic field alignment. J. Am. Chem. Soc. *132*, 17516–17522. https://doi.org/10.1021/ja107309p.

Månsson, M., Nozaki, H., Wikberg, J.M., Prša, K., Sassa, Y., Dahbi, M., Kamazawa, K., Sedlak, K., Watanabe, I., and Sugiyama, J. (2014). Lithium diffusion & magnetism in battery cathode material LixNi1/3Co1/3Mn1/3O2. J. Phys. Conf. Ser. *551*, 012037. https://doi.org/10.1088/1742-6596/551/1/012037.

Melot, B.C., Rousse, G., Chotard, J.N., Ati, M., Rodríguez-Carvajal, J., Kemei, M.C., and Tarascon, J.M. (2011). Magnetic structure and properties of the li-ion battery materials FeSO4F and LiFeSO4F. Chem. Mater. *23*, 2922–2930. https://doi.org/10.1021/cm200465u.

Miura, M., Oshikiri, Y., Sugiyama, A., Morimoto, R., Mogi, I., Miura, M., Takagi, S., Yamauchi, Y., and Aogaki, R. (2017). Magneto-dendrite effect: copper electrodeposition under high magnetic field. Sci. Rep. *7*, 45511. https://doi.org/10.1038/srep45511.

Mogi, I., and Kamiko, M. (1996). Striking effects of magnetic field on the growth morphology of electrochemical deposits. J. Cryst. Growth *166*, 276–280. https://doi.org/10.1016/0022-0248(95)00537-4.

Mohammadi, M., Silletta, E.V., Ilott, A.J., and Jerschow, A. (2019). Diagnosing current distributions in batteries with magnetic resonance imaging. J. Magn. Reson. *309*, 106601. https://doi.org/10.1016/j.jmr.2019.106601.

Mohanta, S., and Fahidy, T.Z. (1972). The effect of a uniform magnetic field on mass transfer in electrolysis. Can. J. Chem. Eng. *50*, 248–253. https://doi.org/10.1002/cjce.5450500219.

Mohanta, S., and Fahidy, T.Z. (1978). Magnetoelectrolysis in non-uniform solenoidal fields. J. Appl. Electrochem. *8*, 265–267. https://doi.org/10.1007/BF00616429.

Monzon, L.M.A., and Coey, J.M.D. (2014). Magnetic fields in electrochemistry: the Kelvin force. A mini-review. Electrochem. Commun. *42*, 42–45. https://doi.org/10.1016/j.elecom.2014.02.005.

Mühlenhoff, S., Mutschke, G., Uhlemann, M., Yang, X., Odenbach, S., Fröhlich, J., and Eckert, K. (2013). On the homogenization of the thickness of Cu deposits by means of MHD convection within small dimension cells. Electrochem. Commun. *36*, 80–83. https://doi.org/10.1016/j.elecom.2013.09.025.

Mukai, K., Aoki, Y., Andreica, D., Amato, A., Watanabe, I., Giblin, S.R., and Sugiyama, J. (2014). Spin fluctuations above 100 K in stoichiometric LiCoO2. J. Phys. Conf. Ser. *551*, 012008. https://doi.org/10.1088/1742-6596/551/1/012008.

Mukai, K., and Inoue, T. (2017). Magnetic susceptibility measurements on Li-intercalated graphite: paramagnetic to diamagnetic transitions in C12Li induced by magnetic field. Carbon *123*, 645–650. https://doi.org/10.1016/j.carbon.2017.08.012.

Mukai, K., Sugiyama, J., and Aoki, Y. (2010). Structural, magnetic, and electrochemical studies on lithium insertion materials LiNi1−xCoxO2 with $0 \leq x \leq 0.25$. J. Solid State Chem. *183*, 1726–1732. https://doi.org/10.1016/j.jssc.2010.05.019.

Mukai, K., Sugiyama, J., Ikedo, Y., Nozaki, H., Shimomura, K., Nishiyama, K., Ariyoshi, K., and Ohzuku, T. (2007). Magnetism and lithium diffusion in LixCoO2 by a muon-spin rotation and relaxation (μ+SR) technique. J. Power Sourc. *174*, 711–715. https://doi.org/10.1016/j.jpowsour.2007.06.111.

Mukai, K., Sugiyama, J., Ikedo, Y., Russo, P.L., Andreica, D., Amato, A., Ariyoshi, K., and Ohzuku, T. (2009). Micro- and macroscopic magnetism in LixNiO2. J. Power Sourc. *189*, 665–668. https://doi.org/10.1016/j.jpowsour.2008.09.069.

Mukai, K., Sugiyama, J., Kamazawa, K., Ikedo, Y., Andreica, D., and Amato, A. (2011). Magnetic properties of the chemically delithiated LixMn2O4 with $0.07 \leq x \leq 1$. J. Solid State Chem. *184*, 1096–1104. https://doi.org/10.1016/j.jssc.2011.03.019.

Neef, C., Wadepohl, H., Meyer, H.-P., and Klingeler, R. (2017). High-pressure optical floating-zone growth of Li(Mn,Fe)PO4 single crystals. J. Cryst. Growth *462*, 50–59. https://doi.org/10.1016/j.jcrysgro.2017.01.046.

Nejat, P., Jomehzadeh, F., Taheri, M.M., Gohari, M., and Abd. Majid, M.Z. (2015). A global review

of energy consumption, CO2 emissions and policy in the residential sector (with an overview of the top ten CO2 emitting countries). Renew. Sustain. Energy Rev. *43*, 843–862. https://doi.org/10.1016/j.rser.2014.11.066.

Nguyen, H., and Clément, R.J. (2020). Rechargeable batteries from the Perspective of the electron spin. ACS Energy Lett. *5*, 3848–3859. https://doi.org/10.1021/acsenergylett.0c02074.

Nitta, N., Wu, F., Lee, J.T., and Yushin, G. (2015). Li-ion battery materials: present and future. Mater. Today *18*, 252–264. https://doi.org/10.1016/j.mattod.2014.10.040.

Nwokeke, U.G., Alcántara, R., Tirado, J.L., Stoyanova, R., and Zhecheva, E. (2011). The electrochemical behavior of low-temperature synthesized FeSn2 nanoparticles as anode materials for Li-ion batteries. J. Power Sourc. *196*, 6768–6771. https://doi.org/10.1016/j.jpowsour.2010.10.071.

Nyman, A. (2011). An Experimental and Theoretical Study of the Mass Transport in Lithium-Ion Battery Electrolytes, doctoral thesis, KTH, School of Chemical Science and Engineering (CHE), Chemical Engineering and Technology, Applied Electrochemistry.

O'Brien, R.N. (2019). The magnetohydrodynamic effect in electrochemical systems including batteries. ECS Trans. *3*, 23–29. https://doi.org/10.1149/1.2795232.

O'Brien, R.N., and Santhanam, K.S.V. (1997). Magnetic field assisted convection in an electrolyte of nonuniform magnetic susceptibility. J. Appl. Electrochem. *27*, 573–578. https://doi.org/10.1023/A:1018402813235.

Ofer, O., Sugiyama, J., Brewer, J.H., Månsson, M., Prša, K., Ansaldo, E.J., Kobayashi, G., and Kanno, R. (2012). The magnetic phase of lithium transition metal phosphates LiMPO4 (M=Mn, Co, Ni) detected by μ+SR. Phys. Proced. *30*, 160–163. https://doi.org/10.1016/j.phpro.2012.04.063.

Ohno, H., Munekata, H., Penney, T., von Molnár, S., and Chang, L.L. (1992). Magnetotransport properties of p-type (In,Mn)As diluted magnetic III-V semiconductors. Phys. Rev. Lett. *68*, 2664–2667. https://doi.org/10.1103/PhysRevLett.68.2664.

Ohno, H., Shen, A., Matsukura, F., Oiwa, A., Endo, A., Katsumoto, S., and Iye, Y. (1996). (Ga,Mn)As: a new diluted magnetic semiconductor based on GaAs. Appl. Phys. Lett. *69*, 363–365. https://doi.org/10.1063/1.118061.

Olivier, A., Chopart, J.-P., Amblard, J., Merienne, E., and Aaboubi, O. (2000). Direct and indirect electrokinetic effect inducing a forced convection. EKHD and MHD transfer functions. A C H Models Chem. *137*, 213–224.

Oz, E., Altin, S., Demirel, S., Bayri, A., Altin, E., Baglayan, O., and Avci, S. (2016). Electrochemical effects and magnetic properties of B substituted LiCoO2: improving Li-battery performance. J. Alloys Comp. *657*, 835–847. https://doi.org/10.1016/j.jallcom.2015.10.080.

Oz, E., Demirel, S., Altin, S., Altin, E., Bayri, A., and Avci, S. (2017). Thermally induced spin state transition in LiCoO2 and its effects on battery performance. Electrochim. Acta *248*, 449–453. https://doi.org/10.1016/j.electacta.2017.07.147.

Panchal, S., Dincer, I., Agelin-Chaab, M., Fraser, R., and Fowler, M. (2017a). Transient electrochemical heat transfer modeling and experimental validation of a large sized LiFePO4/graphite battery. Int. J. Heat Mass Transfer *109*, 1239–1251. https://doi.org/10.1016/j.ijheatmasstransfer.2017.03.005.

Panchal, S., Mcgrory, J., Kong, J., Fraser, R., Fowler, M., Dincer, I., and Agelin-Chaab, M. (2017b). Cycling degradation testing and analysis of a LiFePO4 battery at actual conditions. Int. J. Energy Res. *41*, 2565–2575. https://doi.org/10.1002/er.3837.

Pecher, O., Carretero-González, J., Griffith, K.J., and Grey, C.P. (2017). Materials' methods: NMR in battery research. Chem. Mater. *29*, 213–242. https://doi.org/10.1021/acs.chemmater.6b03183.

Peng, J., Gobet, M., Devany, M., Xu, K., Cresce, A.v.W., Borodin, O., and Greenbaum, S. (2018). Multinuclear magnetic resonance investigation of cation-anion and anion-solvent interactions in carbonate electrolytes. J. Power Sourc. *399*, 215–222. https://doi.org/10.1016/j.jpowsour.2018.07.095.

Personnettaz, P., Landgraf, S., Nimtz, M., Weber, N., and Weier, T. (2019). Mass transport induced asymmetry in charge/discharge behavior of liquid metal batteries. Electrochem. Commun. *105*, 106496. https://doi.org/10.1016/j.elecom.2019.106496.

Philippe, B., Mahmoud, A., Ledeuil, J.B., Sougrati, M.T., Edström, K., Dedryvère, R., Gonbeau, D., and Lippens, P.E. (2014). MnSn2 electrodes for Li-ion batteries: mechanisms at the nano scale and electrode/electrolyte interface. Electrochim. Acta *123*, 72–83. https://doi.org/10.1016/j.electacta.2014.01.010.

Priest, E., and Forbes, T. (2007). Magnetic Reconnection: MHD Theory and Applications (Cambridge University Press).

Rahman, M.M., Wang, J.-Z., Deng, X.-L., Li, Y., and Liu, H.-K. (2009). Hydrothermal synthesis of nanostructured Co3O4 materials under pulsed magnetic field and with an aging technique, and their electrochemical performance as anode for lithium-ion battery. Electrochim. Acta *55*, 504–510. https://doi.org/10.1016/j.electacta.2009.08.068.

Rhen, F.M.F., and Coey, J.M.D. (2007). Magnetic field induced modulation of anodic area: rest potential analysis of Zn and Fe. J. Phys. Chem. C *111*, 3412–3416. https://doi.org/10.1021/jp065393o.

Rhen, F.M.F., Fernandez, D.m., Hinds, G., and Coey, J.M.D. (2006). Influence of a magnetic field on the electrochemical rest potential. J. Electrochem. Soc. *153*, J1. https://doi.org/10.1149/1.2135207.

Ridley, W.E., and Spector, G. (1987). Magnetic Battery (Google Patents).

Rybski, M., Tobola, J., Kaprzyk, S., and Molenda, J. (2018). Electronic structure and magnetism of Lix(Ni-Co-Mn)O2 in view of KKR-CPA calculations. Solid State Ionics *321*, 23–28. https://doi.org/10.1016/j.ssi.2018.03.030.

Salimi, P., Norouzi, O., Pourhoseini, S.E.M., Bartocci, P., Tavasoli, A., Di Maria, F., Pirbazari, S.M., Bidini, G., and Fantozzi, F. (2019). Magnetic biochar obtained through catalytic pyrolysis of macroalgae: a promising anode material for Li-ion batteries. Renew. Energy *140*, 704–714. https://doi.org/10.1016/j.renene.2019.03.077.

Sander, J.S., Erb, R.M., Li, L., Gurijala, A., and Chiang, Y.M. (2016a). High-performance battery electrodes via magnetic templating. Nat. Energy *1*, 16099. https://doi.org/10.1038/nenergy.2016.99. https://www.nature.com/articles/nenergy201699#supplementary-information.

Sander, J.S., Erb, R.M., Li, L., Gurijala, A., and Chiang, Y.M. (2016b). High-performance battery electrodes via magnetic templating. Nat. Energy *1*, 16099. https://doi.org/10.1038/nenergy.2016.99.

Scrosati, B., Hassoun, J., and Sun, Y.-K. (2011). Lithium-ion batteries. A look into the future. Energy Environ. Sci. *4*, 3287–3295. https://doi.org/10.1039/c1ee01388b.

Shen, K., Wang, Z., Bi, X., Ying, Y., Zhang, D., Jin, C., Hou, G., Cao, H., Wu, L., Zheng, G., et al. (2019). Magnetic field–suppressed lithium dendrite growth for stable lithium-metal batteries. Adv. Energy Mater. *9*, 1900260. https://doi.org/10.1002/aenm.201900260.

Shi, F., Pei, A., Vailionis, A., Xie, J., Liu, B., Zhao, J., Gong, Y., and Cui, Y. (2017). Strong texturing of lithium metal in batteries. Proc. Natl. Acad. Sci. U S A *114*, 12138. https://doi.org/10.1073/pnas.1708224114.

Singh, P., Khare, N., and Chaturvedi, P.K. (2018). Li-ion battery ageing model parameter: SEI layer analysis using magnetic field probing. Eng. Sci. Technol. Int. J. *21*, 35–42. https://doi.org/10.1016/j.jestch.2018.01.007.

Song, Y., Zavalij, P.Y., Chernova, N.A., and Whittingham, M.S. (2005). Synthesis, crystal structure, and electrochemical and magnetic study of new iron (III) hydroxyl-phosphates, isostructural with lipscombite. Chem. Mater. *17*, 1139–1147. https://doi.org/10.1021/cm049406r.

Stoeva, Z., Jäger, B., Gomez, R., Messaoudi, S., Yahia, M.B., Rocquefelte, X., Hix, G.B., Wolf, W., Titman, J.J., Gautier, R., et al. (2007). Crystal chemistry and electronic structure of the metallic lithium ion conductor, LiNiN. J. Am. Chem. Soc. *129*, 1912–1920. https://doi.org/10.1021/ja063208e.

Sueptitz, R., Tschulik, K., Uhlemann, M., Gebert, A., and Schultz, L. (2010). Impact of magnetic field gradients on the free corrosion of iron. Electrochim. Acta *55*, 5200–5203. https://doi.org/10.1016/j.electacta.2010.04.039.

Sueptitz, R., Tschulik, K., Uhlemann, M., Schultz, L., and Gebert, A. (2011). Magnetic field effects on the active dissolution of iron. Electrochim. Acta *56*, 5866–5871. https://doi.org/10.1016/j.electacta.2011.04.126.

Sugiyama, J., Nozaki, H., Kamazawa, K., Ofer, O., Månsson, M., Ansaldo, E.J., Brewer, J.H., Chow, K.H., Watanabe, I., Ikedo, Y., et al. (2012). Magnetic and diffusive nature of LiFePO4. Phys.

Proced. *30*, 190–193. https://doi.org/10.1016/j.phpro.2012.04.070.

Suleimanov, N.M., Prabaharan, S.R.S., Khantimerov, S.M., Nizamov, F.A., Michael, M.S., Drulis, H., and Wisniewski, P. (2016). Magnetic order and electronic properties of Li2Mn2(MoO4)3 material for lithium-ion batteries: ESR and magnetic susceptibility studies. Appl. Phys. A *122*, 754. https://doi.org/10.1007/s00339-016-0278-2.

Tacken, R.A., and Janssen, L.J.J. (1995). Applications of magnetoelectrolysis. J. Appl. Electrochem. *25*, 1–5. https://doi.org/10.1007/BF00251257.

Tambio, S.J., Deschamps, M., Sarou-Kanian, V., Etiemble, A., Douillard, T., Maire, E., and Lestriez, B. (2017). Self-diffusion of electrolyte species in model battery electrodes using magic Angle Spinning and pulsed field gradient nuclear magnetic resonance. J. Power Sourc. *362*, 315–322. https://doi.org/10.1016/j.jpowsour.2017.07.010.

Tang, Y., Hong, L., Li, J., Hou, G., Cao, H., Wu, L., Zheng, G., and Wu, Q. (2017). An internal magnetic field strategy to reuse pulverized active materials for high performance: a magnetic three-dimensional ordered macroporous TiO2/CoPt/α-Fe2O3 nanocomposite anode. Chem. Commun. *53*, 5298–5301. https://doi.org/10.1039/C7CC00940B.

Tripathi, B., Kumar, P., Katiyar, R.K., and Katiyar, R.S. (2017). Aligned MWNT channels in free standing polymer nanocomposite as an electrode for Li-ion battery. Appl. Phys. Lett. *110*, 173902. https://doi.org/10.1063/1.4982666.

Uyama, T., Mukai, K., and Yamada, I. (2020). Structure, magnetism, and electrochemistry of LiMg1–xZnxVO4 Spinels with $0 \leq x \leq 1$. Inorg. Chem. *59*, 777–789. https://doi.org/10.1021/acs.inorgchem.9b03058.

Verma, P., Maire, P., and Novák, P. (2010). A review of the features and analyses of the solid electrolyte interphase in Li-ion batteries. Electrochim. Acta *55*, 6332–6341. https://doi.org/10.1016/j.electacta.2010.05.072.

Wang, D., Xin, C., Zhang, M., Bai, J., Zheng, J., Kou, R., Peter Ko, J.Y., Huq, A., Zhong, G., Sun, C.-J., et al. (2019a). Intrinsic role of cationic substitution in tuning Li/Ni mixing in high-Ni layered oxides. Chem. Mater. *31*, 2731–2740. https://doi.org/10.1021/acs.chemmater.8b04673.

Wang, H., Xie, J., Follette, M., Back, T.C., and Amama, P.B. (2016). Magnetic field-induced fabrication of Fe3O4/graphene nanocomposites for enhanced electrode performance in lithium-ion batteries. RSC Adv. *6*, 83117–83125. https://doi.org/10.1039/C6RA17805G.

Wang, L., Menakath, A., Han, F., Wang, Y., Zavalij, P.Y., Gaskell, K.J., Borodin, O., Iuga, D., Brown, S.P., Wang, C., et al. (2019b). Identifying the components of the solid–electrolyte interphase in Li-ion batteries. Nat. Chem. *11*, 789–796. https://doi.org/10.1038/s41557-019-0304-z.

Waskaas, M., and Kharkats, Y.I. (1999). Magnetoconvection phenomena: A mechanism for influence of magnetic fields on electrochemical processes. J. Phys. Chem. B *103*, 4876–4883. https://doi.org/10.1021/jp984730t.

Wei, G., Wei, L., Wang, D., Chen, Y., Tian, Y., Yan, S., Mei, L., and Jiao, J. (2017a). Reversible control of the magnetization of spinel ferrites based electrodes by lithium-ion migration. Sci. Rep. *7*, 12554. https://doi.org/10.1038/s41598-017-12948-6.

Wei, G., Wei, L., Wang, D., Tian, Y., Chen, Y., Yan, S., Mei, L., and Jiao, J. (2017b). Reversible control of the magnetization of Fe3O4 via lithium ions. RSC Adv. *7*, 2644–2649. https://doi.org/10.1039/C6RA26422K.

Wu, C., Yin, P., Zhu, X., OuYang, C., and Xie, Y. (2006). Synthesis of hematite (α-Fe2O3) nanorods: Diameter-size and shape effects on their applications in magnetism, lithium ion battery, and gas sensors. J. Phys. Chem. B *110*, 17806–17812. https://doi.org/10.1021/jp0633906.

Xiao, J., Chernova, N.A., and Whittingham, M.S. (2008). Layered mixed transition metal oxide cathodes with reduced cobalt content for lithium ion batteries. Chem. Mater. *20*, 7454–7464. https://doi.org/10.1021/cm802316d.

Xiao, Y., Liu, T., Liu, J., He, L., Chen, J., Zhang, J., Luo, P., Lu, H., Wang, R., Zhu, W., et al. (2018). Insight into the origin of lithium/nickel ions exchange in layered Li(NixMnyCoz)O2 cathode materials. Nano Energy *49*, 77–85. https://doi.org/10.1016/j.nanoen.2018.04.020.

Xiao, Y., Zhang, F.C., and Han, J.I. (2016). Electrical structures, magnetic polaron and lithium ion dynamics in three transition metal doped LiFe1−xMxPO4 (M=Mn, Co and La) cathode material for Li ion batteries from density functional theory study. Solid State Ionics *294*, 73–81. https://doi.org/10.1016/j.ssi.2016.06.009.

Xiong, Z.-C., Xie, Y., Yi, T.-F., Yu, H.-t., Zhu, Y.-R., and Zeng, Y.-Y. (2014). Effect of lithium extraction on the stabilities, electrochemical properties, and bonding characteristics of LiFePO4 cathode materials: a first-principles investigation. Ceramics Int. *40*, 2655–2661. https://doi.org/10.1016/j.ceramint.2013.10.059.

Yang, C.C., Wu, S.Y., Li, W.H., Lee, K.C., Lynn, J.W., Liu, R.S., and Shen, C.H. (2002). Short-range magnetic correlations in spinel LiMn2O4. Mater. Sci. Eng. B *95*, 162–170. https://doi.org/10.1016/S0921-5107(02)00228-3.

Yoshifumi, T., Hiroshi, Y., Sin-ichi, W., Akio, K., Wenyong, D., and Masao, F. (2000). Effect of high magnetic field on copper deposition from an aqueous solution. Bull. Chem. Soc. Jpn. *73*, 867–872. https://doi.org/10.1246/bcsj.73.867.

Yu, Y.D., Song, Z.L., Ge, H.L., and Wei, G.Y. (2014). Influence of magnetic fields on cobalt electrodeposition. Surf. Eng. *30*, 83–86. https://doi.org/10.1179/1743294413Y.0000000229.

Zhang, J., Zhu, X., Zeng, M., and Fu, L. (2020). Magnetically controlled on-demand switching of batteries. Adv. Sci. *7*, 2000184. https://doi.org/10.1002/advs.202000184.

Zhang, Q., Luo, X., Wang, L., Zhang, L., Khalid, B., Gong, J., and Wu, H. (2016). Lithium-ion battery cycling for magnetism control. Nano Lett. *16*, 583–587. https://doi.org/10.1021/acs.nanolett.5b04276.

Zhang, X., Julien, C.M., Mauger, A., and Gendron, F. (2011). Magnetic analysis of lamellar oxides for Li-ions batteries. Solid State Ionics *188*, 148–155. https://doi.org/10.1016/j.ssi.2010.11.003.

Zhecheva, E., Stoyanova, R., Alcántara, R., Lavela, P., and Tirado, J.-L. (2002). Cation order/disorder in lithium transition-metal oxides as insertion electrodes for lithium-ion batteries. Pure Appl. Chem. *74*, 1885–1894. https://doi.org/10.1351/pac200274101885.

Zheng-Fei Guo, K.P., and Xue-Jin, W. (2016). Electrochromic & magnetic properties of electrode materials for lithium ion batteries. Chin. Phys. B *25*, 17801–17810. https://doi.org/10.1088/1674-1056/25/1/017801.

Zhou, J., Zhang, D., Sun, G., and Chang, C. (2019). B-axis oriented alignment of LiFePO4 monocrystalline platelets by magnetic orientation for a high-performance lithium-ion battery. Solid State Ionics *338*, 96–102. https://doi.org/10.1016/j.ssi.2019.05.002.